Master's degree in Electronic Engineering

Numerical Study of The Variation of Some Electric Properties of Periodic Structures vs Thermal Stimulus

Shabbir Ali

Supervisor
Prof.Ladislau Matekovits

Politecnico di Torino

July 2021

Abstract

Metamaterials (MM) are the marvelous invention of this era because of its great properties. Since than many research has been carried out in this waste field. As it is an artificial material come in existence after tailoring or altering it properties, so it is not found naturally. Moreover,by tuning its properties one can get desired characteristics.

Coefficient of Thermal Expansion (CTE) in MM play an important role. To analyze the CTE, the unit cell model (UCM) is constructed by using copper (Cu) as a material because its CTE is very high. It is the tendency of the material to change its shape by expansion on the specific temperature. The CTE of the material can bring such significant changes in overall dimension. Motivation of this desertion is to investigate the behavior of MM by applying different temperature to the UCM. In this regard, three UCMs are constructed and evaluated one by one by plotting so called Dispersion Diagram (DD). DD is nothing but a relation between frequency of the UCM and phase, it simply states that how much phase shift in UCM has at the specific frequency when a wave propagates from input of the unit cell to its output. At the room temperature, the reference UCM is constructed and DD is evaluated. After that, second UCM is constructed by exploiting co-simulation technique in Computer Simulation Technology microwave studio (CST) and assigned temperature equal to 250℃ utilizing thermal solver and then the same UCM is bring into the mechanical solver to see the CTE due to temperature. It has been observed that the UCM is expended due to temperature then the DD is calculated. Moreover, the DD of both reference UCM and UCM with 250℃ is compared by plotting on the same graph to see the variation of the stop band frequency. Finally, the last UCM with high temperature 1200℃ is (followed same method as it was during UCM 250℃ construction) constructed. It has been examined that the structure is expanded more than UCM 250℃. Hence, its DD is compared with reference UCM to examine the variation of stop band frequency range.

Acronyms and notation

CTE	Coefficient of Thermal Expansion
UCM	Unit cell model
MM	Metamaterial
THz	Terahertz Frequency
Cu	Copper
CST	Computer Simulation Technology Microwave Studio
FIT	Finite Integration Technique
CST MPS	Multiphysics Studio
DD	Dispersion Diagram
FIT	Finite Integration Technique
MMA	Metamaterial Absorber
SNG	Single Negative Metamaterial
DPS	Double Positive Shift

Acknowledgment

Foremost, I humbly thank my God (the most gracious and the most merciful), who blessed me much more than i wished for. I am also very much thankful to my mentor and supervisor Professor Matekovits Ladislau for his motivation, patience and all the necessary support. After his guidance and support i was able to write master dissertation. Beside this, i would like to thank to all my friends.

At the end, I would like to thank my family members for all theirs love and encouragement. My parents who give birth to me and raised me with a love and supported me in all my pursuits.

Table of Contents

List of Figures

List of Table

Chapter 1: Introduction and Historical background

1.1 Introduction

Recent development in the field of science and technology is expend in such a way where everyday life getting smarter from industry to homes, high rise buildings to transport, everything getting smart. This is all due to characteristics of the novel invention of metamaterial. Metamaterial (MM) is a Greek word mean “beyond”. It is an artificial material used to obtain desired property by tailoring or engineering to an application which is not possible to get by natural materials. It is the composition of a sub wavelength made of repeating patten periodically which is called UCM. MMs are made from the combination of different material such as metal, polymer, glass, fiber etc. It has different properties included optical frequency magnetism, negative refractive indices, broad positive refractive indices, impedance matching zero reflection, perfect absorption, or enhanced optical nonlinear properties. Moreover, in the field of optical, every lens made of conventional material was limited due to the frequency of the light uses to focus but due to MM it is now possible to use super lens in which the smallest thing can be seen in the broad way. For the application point of view, the smallest cancer cells can be detected by increasing the resolution of the lens. There are some more advantageous applications of metamaterial included ultra-high resolution imaging systems, cloaking devices, advance antenna, and radar.

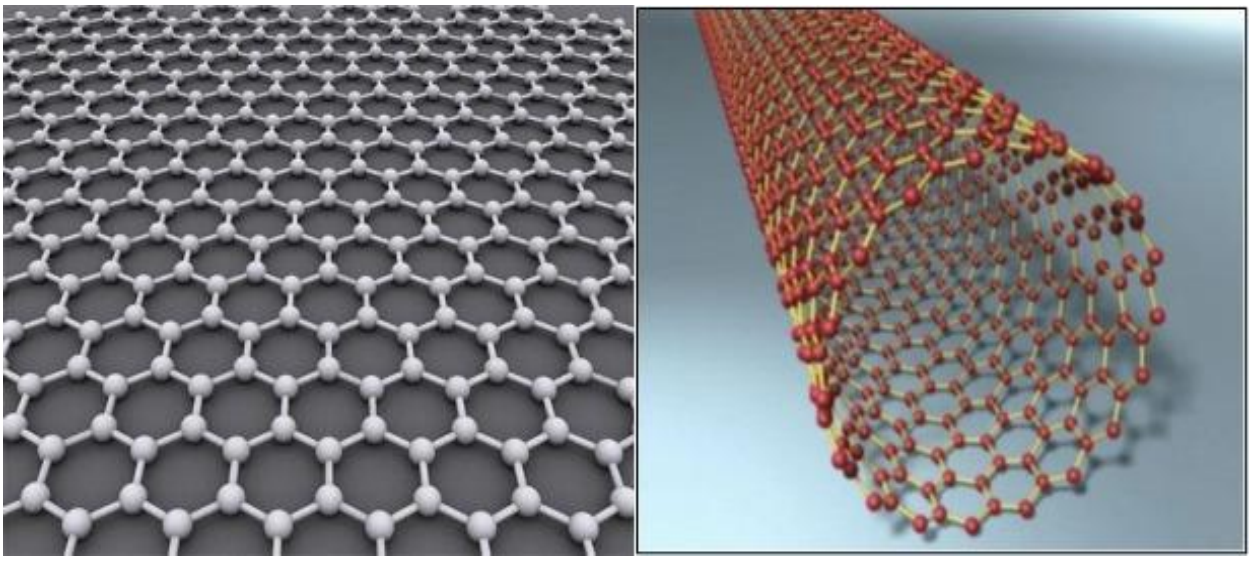

Figure 1.1: Basic Structure of graphene based MM (Xu et al., 2019) [01]

Fig 1. Illustration of a basic structure of MM of graphene sheet, initially one unit cell is made and then repeated several times.

1.2 Background Overview

Metamaterial was first discussed by Russian physicist, Victor Veselago. He proposed the metamaterial theoretically in 1968 (Veselago, 1968) [02], he investigate the structure of the substance negative values of permittivity and permeability simultaneously that how the EM wave travel in such material and what is their properties. However, experimentally it was not possible to achieve negative values of permeability and permittivity until discovered by John B.Pendry et al in 1996 (John B Pendry, Holden, Robbins, & Stewart, 1999) [03], he proposed that an electromagnetic response of the permittivity materials can be generated by a periodic array of copper wire with a specific gap and radius. He also said that periodic array of split ting resonators could have band gap frequency where the value of permeability is negative.

1.3 Personal contribution in the dissertation

At the very first step, different materials were considered and found copper (Cu) amongst all on top. After material selection, different geometry structure was considered to constructed reference UCM, so initially the first geometry of UCM was considered in that geometry an small sphere is placed at the center of two metal plates (top and bottom) made by same material as

whole UCM is made with a single material which is copper. In the second consideration the cube was inserted instead of sphere and this last one is selected to be implement throughout the research. So finally, three UCM were constructed (first Reference UCM at room temperature, second UCM with temperature 250℃ and the third UCM with 1200℃ temperature) to evaluate dispersion diagram (DD) by using Brillion zone in CST software (Gamma to X, X to M and M to Gamma). DD of each UCM is evaluated separately and then comparison is carried out of DD of all UCMs. Moreover, by exploiting marvelous features of CST called Multiphysics, thermal solver is used along with mechanical solver. In thermal solver the source is assigned to UCM and this UCM was then bring into mechanical solver to see the thermal expansion of the model due to temperature (which was assigned in the thermal solver). Dispersion diagrams of all the UCMs were compared and examined that there are tunability, it has been observed that the lower order modes reasonably all right, but the higher order modes are not in ordered. There are many possibilities for future work in this topic or research.

1.4 Recent interest in metamaterial and applications

In the 1967, Vaselago published a paper which got considerable amount of interest at that time. However, the real metamaterial research did not start until about three decades later when many seminal paper were issued (Smith, Padilla, Vier, Nemat-Nasser, & Schultz, 2000) [04] (John Brian Pendry, 2000) [05] (Smith & Kroll, 2000) [06]. Metamaterial is being utilizing in many application (Oliveri, Werner, & Massa, 2015) [07], some marvelous applications are antenna and waveguide engineering, sensing (Alves, Grbovic, Kearney, Lavrik, & Karunasiri, 2013) [08] (Liu, Fan, Ku, & Mao, 2016) [09], imaging (Wilbert, Hokmabadi, Martinez, Kung, & Kim, 2013) [10] (Carranza, Grant, Gough, & Cumming, 2016)[11] and absorbing and manipulating electromagnetic wave (EM), microscopy sensing and light manipulation.

Some potential applications have been adopted such as thermally tunable MM absorber of EM at different frequency ranges (MHz to THz). There are different kinds of application and tunable metamaterial is on top, with its special kind of properties of absorption of EM. The mechanism of absorption is that,the EM field should be strongly confined inside lossy material. It is possible to achieve absorption by realizing different types of structures such as periodic

structure and Salisbury and many more. (Thongrattanasiri, Koppens, & De Abajo, 2012) [12]. The structure of the absorber can be construct by the mixture of different materials such as strontium titanate with copper ring as a top layer and FR4 on middle and copper film at the bottom, graphene layer etc. At 300K, absorption can reach almost 96% at 684 MHz in the P band frequencies (L. Wang et al., 2019) [13]. On the contrary, it reached 99.9% in terahertz at 2.48 THz frequency when the temperature was 400k (Huang et al., 2019) [14].

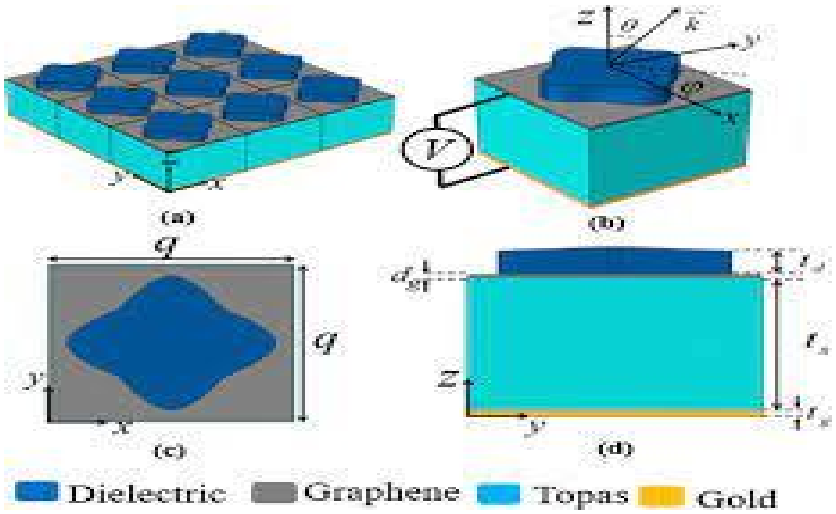

Figure 1.2: Absorber Structure with different Materials(Nourbakhsh, Zareian-Jahromi, Basiri, & Mashayekhi, 2020) [15]

The absorption can be calculated on different temperature ranges in the CST MWS (Elwi, 2019 #71) [16].

1.5 Outline of Dissertation

There are four chapters as follow:

- In Chapter 1 an introduction along with historical overview and a discussion on the most recent interest in metamaterial applications are given.
- In the Chapter 2 a brief introduction about Metamaterials, Electromagnetic metamaterial (Basic principle of electromagnetic radiation based on maxwell equation) and different classification of metamaterial for example negative refractive index (NIM), double positive media (DNG), single negative media (SNG), electromagnetic

bandgap, bi-isotropic material and chiral metamaterial, Moreover, we have discussed about different types of metamaterial such as Terahertz, Photonic, Tunable and Plasmonic Metamaterials. We have some marvelous applications like Metamaterial Antenna, cloaking devices and Super lens.

- In Chapter 3 the implementation and approach is discussed briefly, start from the material selection and then construction of UCM by using CST MWS software. Moreover, some other features of CST MWS are used during desertion to know how the structure is given temperature and how the CTE is calculated by using thermal solver and mechanical solver, respectively. As per requirement of the research to see the behavior of frequency vs phase the so-called DD is analyzed for the three UCM individually. Very brief introduction is provided about DD, thermal solver, and mechanical solver. Step by step results are introduced.
- In Chapter 4 the results are analyzed briefly by comparing UCM having 250℃ temperatures with the reference UCM. The CTE in the UCM of 250℃ due to temperature is observed some tends of millimeter (mm) with respect to reference UCM. Similarly, another comparison is carried out having 1200℃ UCM with reference UCM and all the results are summarized in the form of Table where all the data of given UCM is compared. At First, the DD of reference UCM and the DD of UCM with 250℃ is analyzed by plot together, similarly the DD of reference UCM is compare with UCM having 1200℃ temperatures by plotting on the same graph.

Chapter 2: Metamaterial

2.1 Metamaterial

MMs are called man-mad materials that have not only electromagnetic but thermal and acoustic characteristics that are not found in nature, such as electromagnetic cloaking or refraction. As it has been discussed in the introduction that in 1960, Victor Veselago first talked about MM properties (Veselago, 1968) [2], his research mainly focused on the idea of negative index materials later on his research come in reality after some years. MM is made up of unit cells, which are often tiny elements also known as meta-atoms, each of which is significantly smaller than the wavelength. UCMs are constructed microscopically using common material such as polymers, dielectrics, and metals. Their precise form, size, geometry, orientation, and arrangement can macroscopically effect light in unique ways, such as generating resonances or unique macroscopic permittivity and permeability values. Negative index metamaterial and chiral metamaterials are examples of existing MM (Wang, 2009) [17], plasmonic metamaterials (Yao, 2014) [18], photonic metamaterials (Feng, 2020) [19] etc. Due to the nature of their subwavelength, those MMs operate at microwave frequencies have a size of unit cell of some millimeters, while on the other hand, unit cell size of MM working in the visible spectrum is typically a few nanometers. In addition, MM are intrinsically resonant, meaning that they can powerfully absorb light at a restricted range of frequencies that can block or absorb a certain color in the spectrum. The reaction of the atoms or particles that make up the material to an electromagnetic wave passing through determines EM properties such as electric permittivity (ε) magnetic permeability (μ) in conventional materials. At the atomic level, EM properties are not determined. Instead, the configuration of a group of a smaller particle that make up the metamaterial determines these characteristics.

2.2 Maxwell's Equations

EM theory is the most important part of physics, which is behind of the MM. Start with the equation of Maxwell's. In 1865, the James Clerk Maxwell published these equations. While Maxwell's equation comes in many forms, for example linear, isotropic etc. However, some

basic equation described here.

$$\bar{\nabla} \cdot \bar{D} = 0 \tag{2.1}$$

$$\bar{\nabla} \cdot \bar{B} = 0 \tag{2.2}$$

$$\bar{\nabla} x \bar{E} = -\frac{\partial \bar{B}}{\partial t} \tag{2.3}$$

$$\bar{\nabla} x \bar{E} = -\frac{\partial \bar{D}}{\partial t} \tag{2.4}$$

where $\bar{B}$ is the magnetic field and $\bar{E}$ electric while $\bar{D}$ is the displacement of electric and $\vec{\mathrm{H}}$ is the strength of magnetic field.

$$\bar{E}\,(r,t) = \begin{bmatrix} E \\ B \end{bmatrix} \mathrm{ei}\,(\bar{K} r - \omega t) \tag{2.5}$$

$$\bar{B}(r,t) = \begin{bmatrix} E \\ B \end{bmatrix} \mathrm{ei}\,(\bar{K} r - \omega t) \tag{2.6}$$

putting this form into Maxwell equations, so E and B are not mutually perpendicular but also perpendicular to the wavevector $\bar{K}$. The dealing of transverse EM with wavevector $\bar{K}$ and angular frequency ω. Here the relation is used which provide a connection between incident fields and the corresponding polarization (P) and magnetization (M)

$$\mathrm{D} = \varepsilon_0 \bar{\mathrm{E}} + P = \varepsilon_0 (1 + \chi e)\, \bar{\mathrm{E}} = \varepsilon_r \varepsilon_0\, \bar{\mathrm{E}} = \varepsilon\, \bar{\mathrm{E}} \tag{2.7}$$

$$B = \mu_0 (\vec{\mathrm{H}} + M) = \mu_0 (1 + \chi m)\, \vec{\mathrm{H}} = \mu_r\, \mu_0 \vec{\mathrm{H}} = \mu \vec{\mathrm{H}} \tag{2.8}$$

On the above equation the magnetic susceptibility (χe, χm) the electric permittivity, absolute,

free space and relative (ε_0, ε, ε_r), and the magnetic permittivity absolute, free space and relative (μ_0, μ, μ_r). All of these will be complex and dispersive means function of frequency.

$$\varepsilon = \tilde{\varepsilon}(\omega) = \varepsilon_1(\omega) + i\,\varepsilon_2(\omega) \text{ and } \mu = \mu(\omega) = \mu_1(\omega) + i\mu_2(\omega) \quad (2.9)$$

Furthermore, the frequency dependence and complex nature of the parameters will not always be explicitly stated. We can define additional material parameters using the permittivity and the permeability. The index of refraction(n), the wave impedance (Z) and the conductivity (σ):

$$\boldsymbol{n = \sqrt{\varepsilon r r}} \quad (2.10)$$

$$\boldsymbol{z = \sqrt{\mu/\varepsilon}} \quad (2.11)$$

$$\boldsymbol{\sigma = i\omega(\varepsilon_0 - \varepsilon)} \quad (2.12)$$

Where all the above parameters include with real and imaginary component and dependent on frequency.

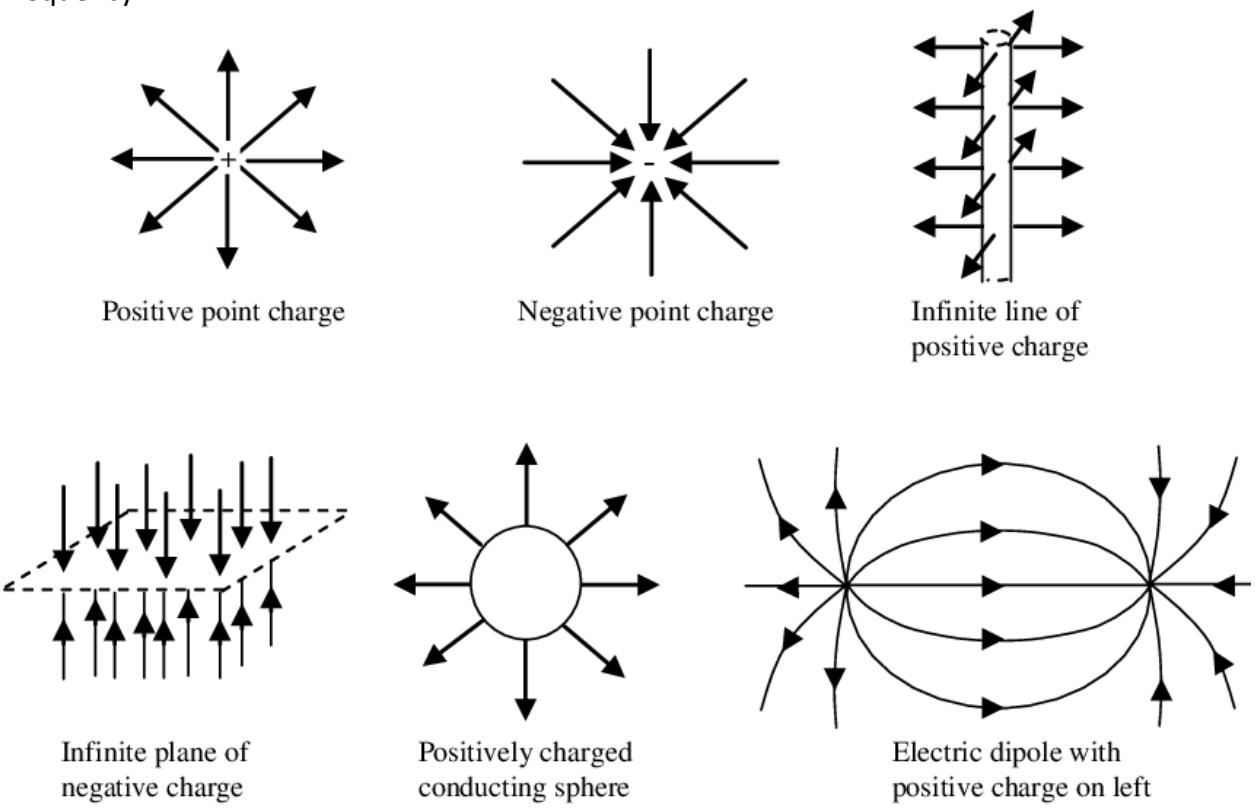

Figure 2.1: Maxwell's Equation Electric Field Orientation (Fleisch, 2008) [20]

2.3 Metamaterial Classification

In 1967, the presence of homogeneous substances of negative permittivity ε and permeability μ firstly discussed by Veselago. He stated that, there are four kinds of substances which are technically considered according to the values of ε and μ. As can be seen in the picture that there are four quadrants with certain values of magnetic permeability μ and electric permittivity ε. Lets discuss all of them one by one.

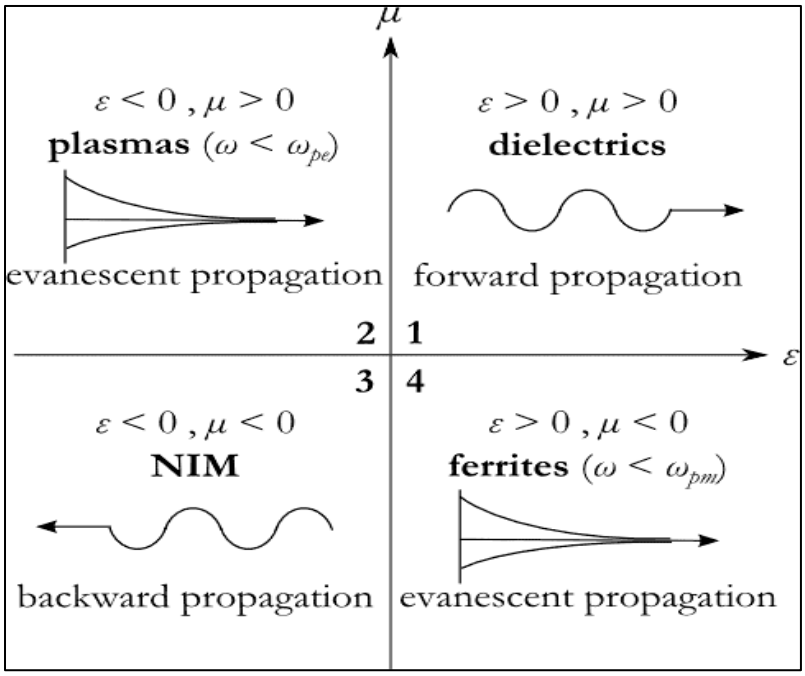

Figure 2.2: Permeability and Permittivity Diagram

2.3.1 Negative Refractive Index

It is the advantage of MM to build a structure with negative refractive index because this marvelous property does not found in any non-synthetic material. Materials that are found in photonic for example water or glass, their permeability μ and permittivity ε are positive values. Moreover, at the visible wavelength, metal either gold or silver has negative permittivity ε. As we know that any material that have negative permeability or permittivity but not both, are invisible to EM radiation. Figure-5 shows the refraction in conventional material and left-

handed metamaterial. All of them are well known by transparent non-MM having a positive permeability or permittivity. For convenient, the positive square root is used for ***n***. moreover, some engineered MMs have negative permeability and negative permittivity. The product of both is positive and whereas ***n*** is real. In some cases, it is essential to take the negative square root for ***n***. Physicist Victor Veselago proved that such substances can transmit light. It is also called double negative metamaterial (DNG) (Iyer, 2002) [21].

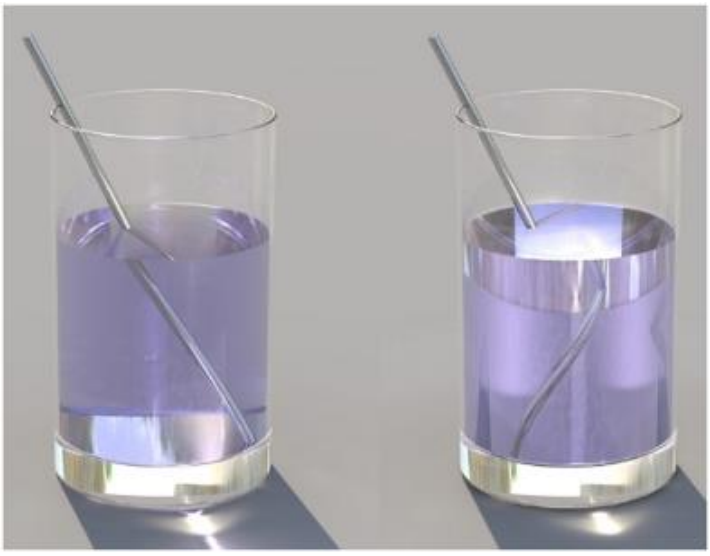

Figure 2.3: Conventional Material without refraction and refraction in left-handed metamaterial [22]

2.3.2 Double Positive Medium (DPS)

When both the values of μ and ε are positive in the material it is called double positive, which are conventional material or also known transparent. This material is occurring in nature such as naturally accruing dielectric. In DPS, electromagnetic wave propagates in forward direction (Pearson, 2016) [23].

2.3.3 Single Negative Metamaterial (SNG)

In this classification either electric permeability (μ) permittivity (ε) is negative (ε<0 or μ<0). SNG is also called epsilon negative media which mean the μ is positive and ε is negative. As SNG media is dispersive so their μ and ε will be change if frequency is change. They will act like DNG if they are joint (Alù, 2007) [24].

2.3.4 Electromagnetic Bandgap metamaterial

Another marvelous class is Electromagnetic Bandgap Metamaterial. This is achieved with a class of MM known as photonic crystals (PC) and left-handed materials. They are the novel class of artificially engineered structure, and both control and manipulate the propagation of electromagnetic waves (Engheta, 2006) [25].

2.3.5 Bi-isotropic and bi-Anisotropic

Normally it is thinking that the MM has magnetic and electric response separately by permittivity and permeability when they categorize MM into SNG or DNG but that is not true. In most of the cases, the magnetic field induce electric polarization while the electric field cause magnetic polarization. It is called Bi-isotropic. Media that showing magnetoelectric coupling and that are anisotropic as called bi-anisotropic (Kriegler, 2009) [26].

2.3.6 Chiral Metamaterial

The word chirality means “handedness” was first used by Lord Kelvin in 1873 (B. Wang et al., 2009) [17]. Chiral medium particles cannot be superimposed on their mirror images. Due to the inherent chiral asymmetry of the medium, it has a different response to a right circularly polarized wave and left circularly polarized. Moreover, there is cross coupling between the magnetic and electric field passing through the chiral medium. The cross-coupling effects is described by a dimension less permitter k. the refractive indices of right circularly polarized and left circularly polarized wave is vary in the existence of k. In the early 19^{th}, it is suggested by Biot that the phenomenon has root in the molecules. In addition, the phenomenon of optical activity is introduced into radio waves in visible light, which contains a set of helical coils that act as artificial chiral molecules.

2.4 Types of Metamaterials

2.4.1 Terahertz Metamaterial

This is the class of composite MM designed to interact with terahertz frequency (THz) frequency range. The THz waves are larger than microwave but lower than visible light. With these characteristics it is difficult to influence THz radiation in conventional electronic components and devices. THz frequency or submillimeter wavelength in between of microwave and infrared wavelength. This frequency range is difficult to approach because of the strong atmospheric attenuation (Armstrong, 2012) [27]. Moreover, there is some lack in devices for example sources, detector and modulators that functional in infrared as effectively as their counterparts (Williams, 2005) [28]. However, there are many potential device applications that can take advantage of this part of the electromagnetic system, such as shielding detection, weather navigation, and skin cancer detection. In the year of 2004, split ring resonator model was scaled to be subwavelength from a periodicity of 10 mm to 36.5um in THz regime and a good magnetic response of almost 1 THz can be obtained without any additional engineering; the structure shows almost the same magnitude on the frequency scale, three times higher than its counterpart. The versatility of this design promotes the development of terahertz metamaterial facilities, such as modulators, sensors, and active space masks (Watts, 2015) [29].

2.4.2 Photonic Metamaterial

Photonic metamaterials are also called optical MM, it is the type of electromagnetic MM that interact with infrared, visible wavelength, and cover THz range. Photonic MM can be described as a combination of two different types of material optical and optical band gap material. Photonic MM is a material whose optical properties are derived from artificial structural units with partial wavelength units, such as nanowires.

The optical properties can be described by its refractive index (n) which could be 1, the artificial isotropic cell can be created which have magnetic and electric reaction. The largest photonic spectrum in millimeters (mm) is about 2 mm from the visible to the near infrared, and inclusion is typically approximately 1.5 times greater than the wavelength of light. These characteristics are essential for the use of MM in a wide range of optical applications in high-performance photonics applications (Litchinitser, 2008) [30].

2.4.3 Tunable Metamaterial

The tunable MMs are those materials in which we have different response when the EM wave interacts with a material. In tunable MM frequency can be changed according to requirement. The capability of tunable MM is to be absorbed, reflected, and transmitted the EM wave. However, the lattice configuration of the tunable MM is dynamic in real time allowing the MM system to be reconfigured during operation. This involves advances by developing different forms of MM beyond the bandwidth limits of left-handed materials (Huang, 2019) [31].

2.4.4 Plasmonic Metamaterial

Plasmonic MMs are the artificial materials typically composed of noble metals in which the features of electronic and photonic are linked by coupling photons to conductions of metal also known as surface plasmon. This rationally constructed systems have notably attracted as they have certain interesting properties that cannot be accomplished with naturally occurring materials. Perfect absorption of light is one of the recent exotic properties of plasmonic MM which has broadened its application area considerably. This is achieved by constructing a medium whose impedance though opaque matches that of free space. If such a medium is filled with some lossy medium, the resulting structure can absorb light totally in a sharp or broad frequency range (Yao, 2014) [18].

2.5 Applications of Metamaterial

2.5.1 Metamaterial Antenna

To enhance the performance of the system MM antennas are used. Antenna radiated power can be enhanced by MM. Moreover, MMs have negative permeability properties for example high directivity, tunable operational frequency, and smaller size of antenna (Dong, 2012) [32]..
For a type of MM exhibiting negative dielectric constant and negative permeability, it is expected that the antenna performance will be significantly improved. Antennas made of MM has great advantage of bandwidth limitation efficiency as compared to those antennas made of conventional material. The MM antenna will allow smaller components to cover a wider frequency range by making better use of the small space and the available space of the platform. The MM used in the ground plane around the antenna provides better isolation

between the RF or microwave channels of the antenna array (MIMO) (Multiple input, multiple output). To improve radiation efficiency, high impedance ground plane can also be used. MMs have also been used to increase the beam scanning range by using both forward and backward waves in leaky wave antennas. Various MM antenna systems can be used to support surveillance sensors, communication links, navigation systems, command, and control systems (Dong, 2012) [32].

2.5.2 Cloaking Devices

The metamaterial cloaking device is a fictional or hypothetical low observation technology, it is the simple process in which the scattered electromagnetic field is canceled from an arbitrary shaped object, this is accomplished by using a shield that covers the object, which allows the complete absorption of scattering for all of the observation angle in far or near field (Forouzmand & Yakovlev, 2015) [33]. Moreover, this phenomenon can be realized another way when a light ray going through the cloak would enter the observer at the same time as a ray travelling through an empty space at the same time. Science a diverted light takes a longer path, the speed of light in the vacuum should be surpassed but it would contradict the theory of Einstein's special relativity. If the clock works on narrow bandwidth the violation will no longer valid (Smith, 2014) [34]. There are many ways to approaching cloaking, for example transformation optics is the phenomenon in which an electromagnetic waves are manipulated in such a way that cloak bends the wave around the object (Forouzmand & Yakovlev, 2015) [33]. Plasmonic cloaking uses a homogeneous sheet of dielectric constant negative or near zero canceling the polarization currents of the hidden objects (Farhat et al., 2015) [35]. Mantle cloaking the goal is to compensate for the dispersion of a given object using artificial material with proper surface impedance values.

2.5.3 Super lens

According to the new study, super-lens is so powerful which allow scientist to detect germs on zero level which was not possible by conventional material. Since many years, microscopes help researchers to make important discoveries, such as providing the presence of microbes.

Due to the physical laws of light, it restricts conventional lenses from exceeding their limits, which means they can only focus on elements that are not less than half the wavelength of light

that these objects can see. It means that normal lenses in traditional optical microscopes are limited to examining items that are about 200 nm or billions of meters in size about the size of smallest bacteria. In the last ten years, researchers have created super lenses. Million spherical beads of titanium dioxide comprise the new super lens. Each bead consists of 15 nanometers wide applied to desired material to view. Related titanium dioxide nanoparticles are now also present in sunscreen products and white paint. The shape, size and material of these particles and their relative position to each other help them work together, just like a lens, before there was no magnification function in the ordinary lens. This super lens will increase the magnification of current microscopes by a factor of around five. Researchers were able to generate sharp images of objects 45 nm in scale. Due to advancement in the super lens the smallest virus or germs can be visualize that were previously invisible. The advantage of the super lens observed by the researchers is that titanium dioxide is cheap and easily available. The super lens can be applied to any content anyone wants to see, meaning researchers do not need to buy a new microscope (Haxha, 2018) [36].

Chapter 3: Implementation and Approach

3.1 Material Selection

Let us start from the material selection, at the beginning of the research the properties of the several materials have been investigated, in terms of CTE. In this regard the investigation was carried out in two main categories Metal and Dielectric. The copper is selected among. All the materials have been summarized in the table form.

3.2 Metals with high CTE

S.no	Material symbol	Classes Material	Coefficient of thermal expansion (CTE) x10-6/K at 20℃
1.	Cd	Cadmium	30.8
2.	Zn	Zinc	30.2
3.	Pb	Lead	29
4.	Al	Aluminium	23.1
5.	Ca	Calcium	22.3
6.	Sn	Tin	22.0
7.	Mn	Manganese	21.7
8.	Cu	Brass	19
9.	Ag	Silver	18.9
10.	SUS304	Stainless steel	17.3
11.	Cu	Copper	17
12.	Au	Gold	14.2
13.	Ni	Nickel	13.4
14.	Fe	Steel	13.0
15.	Co	Cobalt	13.0
16.	Fe	Iron	11.8
17.	Pd	Palladium	11.8
18.	Be	Beryllium	11.3
19.	Pt	Platinum	8.8
20.	Ti	Titanium	8.6
21.	V	Vanadium	8.4
22.	Nb	Niobium	7.1
23.	Ni	Niobium	7
24.	Ta	Tantalum	6.4
25.	W	Tungsten	4.5

Table 3.1 Metal properties with high coefficient of thermal expansion CTE

3.3 Dielectric materials with high CTE

S.no	Material symbol	Classes Material	Coefficient of thermal expansion (CTE) x10-6/K at 20℃
1.	PP	Polypropylene	150
2.	PVC	PVC	52
4.	ZrO2	Zirconia	9.7
5.	Glass	Glass	8.5
6.	Al2O3	Alumina	8.1
7.	Si3N4	Silicon nitride	6
8.	Ge	Germanium	5.9
9.	AlN	Aluminum nitride	5.6
10.	SiC	Silicon carbide	2.77
11.	Si	Silicon	2.56

Table 3.2: Dielectric Materials properties with high CTE

3.4 Copper

Metal has been chosen to investigate and so it is decided to employ Copper as material to be used for further investigation. Copper (Cu) has been using since many years. It is a material element having a very high CTE and the electrical conductivity. It is one of the few metals that can occurs in nature in a directly usable form, just because of these marvelous properties of novel material, it has been decided to use it as the basic material.

3.5 Simulation Software: CST MWS Studio Suite

3.5.1 Why Simulation?

Simulation is the limitation of the operation of a real-world system over time. Models are used by the simulation because it represents the overall behavior of the system, that's why people are adopting this technology before designing a final model to save manufacturing cost, to avoiding errors in the physical design of the system.

3.5.2 CST Microwave Studio Suites

It is a simulation software which is widely used for antenna application.it is well known for the EM simulation of high frequency components. The working principle of CST MICROWAVE STUDIO (CST) is based on Finite Integration Technique (FIT). There are two main domains in which CST carry out simulation as called Time domain and Frequency domain. The accuracy of this software is beyond the limitation. Several days simulation shrinks to few hours which is another advantage of this software. There are different types of simulation modules available in CST but only 3D Simulation is of our interest.

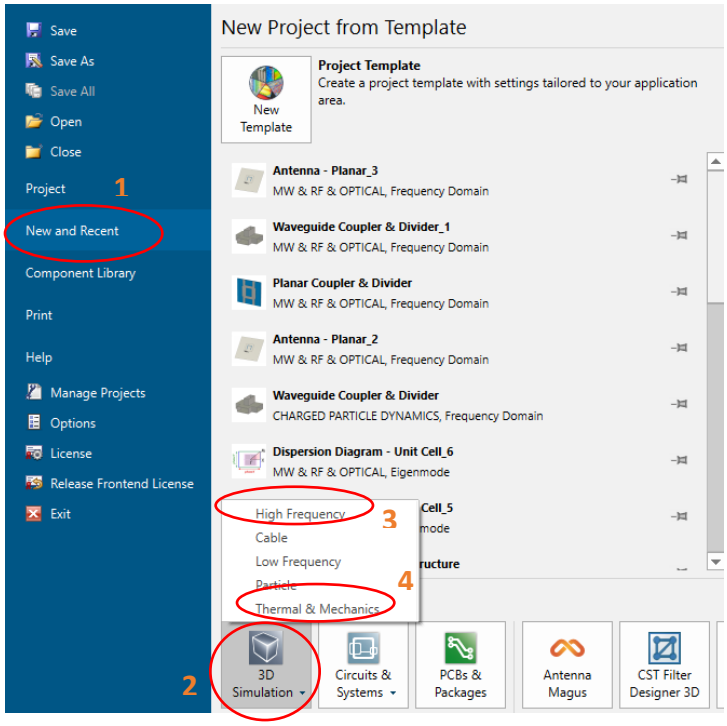

Figure 3.1: Main window of CST

The structure under investigation is more examined by using the marvelous feature of CST software called CST Multiphysics Studio or (CST MPS). Just like EM High frequency solver, similarly Multiphysics consist of two main and important solver called Thermal Solver and Mechanical Solver.

3.5.3 CST Multiphysics Studio (CST MPS)

It is a powerful and easy to use tool for the analysis of thermal and mechanical stress and CTE. Multiphysics simulation is widely known by its feature called “co-simulation or coupled EM simulation” which means different simulation solver can be interlink together under the roof of Multiphysics to save simulation time, for the understating point of view, one can interlink its CST EM solver frequency task to Multiphysics for thermal expansion analysis or mechanical stress and strain and then the results can also be fed back to EM solver for further analysis. Moreover, just like EM solver, CST particle studio can be coupled with CST MPS. Thermal and mechanical solver are the feature of MPS [37].

3.5.4 Thermal Solver Analysis

The thermal analysis is the part of MPS and widely used for assigning temperature by temperature source. The temperature changes in the structure can be modeled and the heat flow into the structure to test the performance of heat sink for make sure the reliability of components sensitive with temperature. In addition, thermal solver dealt with bioheat effects to know how the field is interact with the body.

3.5.5 Mechanical Solver Analysis

The mechanical analysis is the novel part of CST MPS. It is utilized for calculate the deformation. Strain and stress and finally CTE due to temperature.

3.6 Dispersion Diagram Brillouin Zone

As we are interested to investigate the behavior of our UCM related with band gap. To describe the propagation of electromagnetic waves, k is an important wave number. Mostly in lossless case the wave number k is equal to phase constant k=β. In certain cases, phase constant (β) is a function of frequency (ω). when the phase constant is found, the group velocity and phase velocity can be calculated:

$$vp = \frac{\omega}{\beta}, vg = \frac{d\omega}{d\beta} \tag{3.1}$$

Field distribution, for example field changes literally, may also be measured. The relationship

between β and ω is a linear function of a plane wave in free space.

$$\beta(\omega) = k = \omega\sqrt{\mu o\, \varepsilon} \tag{3.2}$$

For surface waves propagating in the structure, it is usually difficult to give a clear expression for the wave number k. To find the wave number, you need to solve a unique value equation or run a global wave simulation. It is necessary to note, an eigen-value equation's solution may not be unique. In other words, at the same wavelength, there may be many different propagation constant [38].

In the DD with a two-dimensional periodic structure, a unique description of the frequency dispersion effect of the phase change in the three main direction of the surface wave, which are Γ to X, X to M, and M to Γ as in the Fig 3.2.

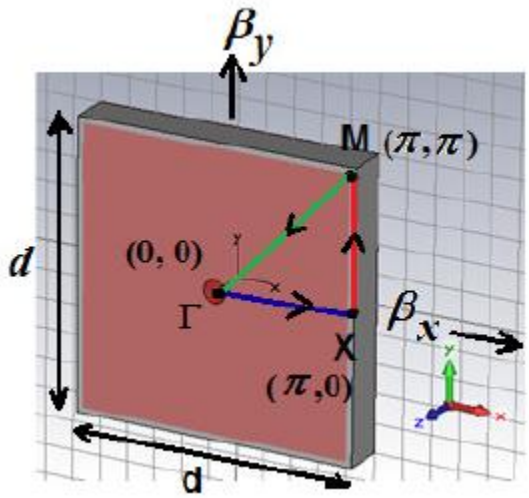

Figure 3.2 Definition of a 2D-periodic structure

3.7 Designing of Unit Cell Model and approach

The UCM under consideration is used to examine its thermal behavior at different temperature range. The copper (Cu) as material is employed to build UCM because its CTE is so high almost α=17(x10-6/K). It is the tendency of the metal to change its shape, area and volume at required temperature, to know its behavior the UCM is evaluated in three main scenario as follow: the first UCM examined without temperature called reference UCM, second UCM with temperature 250℃ and last UCM with high temperature such as 1200℃. At

the first instance, the DD of reference UCM is evaluated then the second UCM having temperature of 250℃ is evaluated by calculating DD. At the end, the last UCM having temperature 1200℃ is evaluated through DD. Moreover, the DD of both the UCM (250℃ and 1200℃) is compared one by one with DD of reference UCM to analyzed what sort of change occurred due to temperature.

3.8 Reference Unit Cell Model

To see the behavior of the reference UCM at room temperature, simply the model is constructed by copper as a periodic structure composed of two square planes symmetrically (both have same height, width and length), one plane is placed at the ground and the second one placed at the top, both planes are connected by via with a distance of 15 millimeters (mm). Moreover, the small box is placed at the middle of the via. This simple structure can be observed in Fig 3.3.

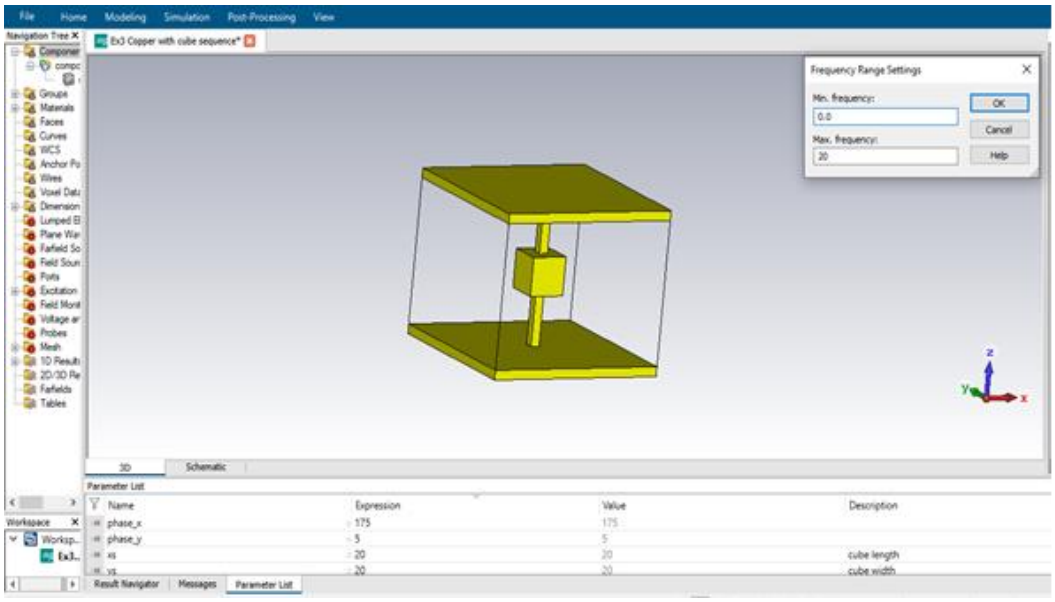

Figure 3.3 Basic UCM model

All the dimensions are in the order of millimeter (mm) and frequency range from 0 GHz to 20 GHz is adopted throughout the structure.

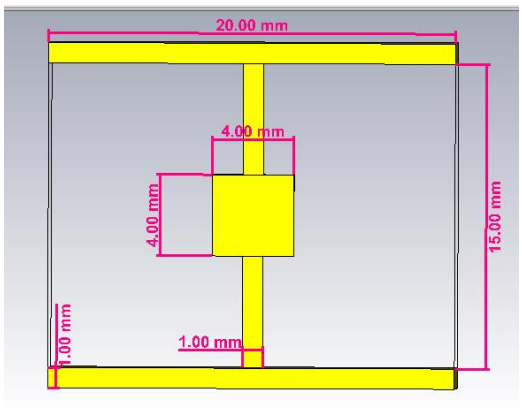

Figure 3.4. Detailed information of reference UCM

In the Tab 3.3, all the required information related to dimension and coordinates of the structure is presented in detail.

Grounded Square Plane and Top Square Plane (mm)			
Length	-10 to 10	X min to X max	Total length 20
Width	-10 to 10	Y min to Y max	Total length 20
Height	0.0 to 1.0	Z min to Z max	Total thickness 1.0
Via (connected ground to top) (mm)			
Length	-0.5 to 0.5	X min to X max	Total length 1
Width	-0.5 to 0.5	Y min to Y max	Total length 1
Height	0.0 to 15	Z min to Z max	Total height 15
Square Brick (connected with via) (mm)			
Length	-2.0 to 2.0	X min to X max	Total length 4
Width	-2.0 to 2.0	Y min to Y max	Total length 4
Height	-2.0 to 2.0	Z min to Z max	Total height 4

Table 3.3. The dimension details of the model

3.9 Frequency Setting: 0-20 GHz

3.10 Boundary condition

The boundary condition for x axis and y axis plane are used as an “electric” Et=0 whereas for the z axis is defined as “periodic”. Moreover, the phase shift is also defined to the periodic boundary so that the phase shift can be used for parameter sweep, to find out the current structural frequency dispersion behavior. As the investigation of interest was to quantify the deformation that’s why mechanical facets are considered.

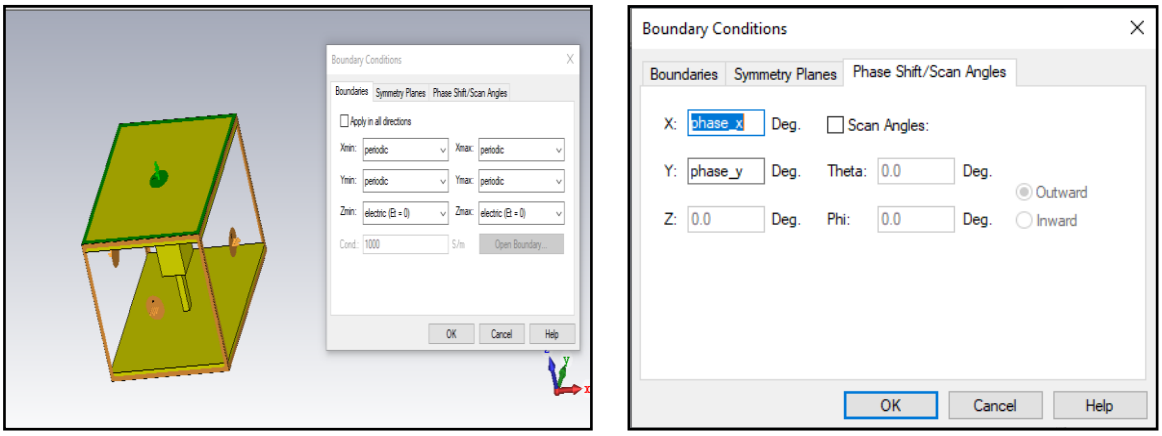

Figure 3.5 Boundary condition of the model

The goal of the investigation of specific model (reference UCM) is to see its behavior of frequency vs phase by plotting so called DD. To do so, all the primary setting was done by setting boundary condition, assigning frequency starting from 0-20 (GHz) and in the background setting material type was normal. The DD can be calculated only on in eigen mode solver, as higher number of modes were interest so 10 number of modes selected along with tetrahedral mesh type because tetrahedral is faster than hexahedral.

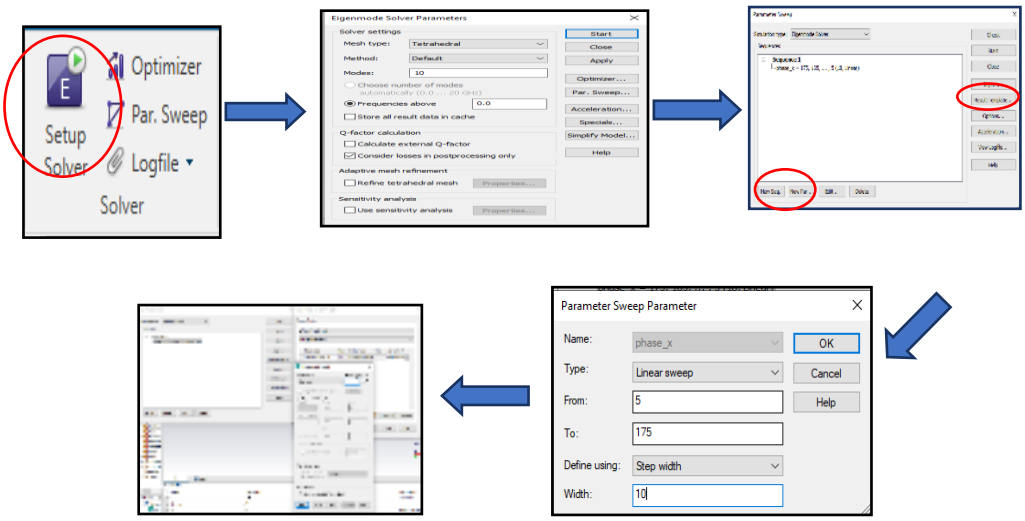

Figure 3.6 Setup of DD

In the Fig 3.6 to calculate DD some sort of setting needed, as it has been mentioned above that the eigen mode is only the solver in which DD is calculated so by selecting eigen mode the tetrahedral mesh type is selected because of its simulation speed. After that, 10 number of modes assigned. Exploiting Brillion zone property to calculate DD are as follow.

3.10.1 Γ TO X

This is the first set of Brillion zone in which the phase constant along x-axis is defined from 5 to 175 degree with step width of 10 while the phase_y is set to 5 degrees. Only 10 number of modes were interest so first set is calculated. We start from 5 degrees to 175 degrees instead of 0 to 180 degrees to avoid long simulation duration.

3.10.2 X TO M

This is the second edge of the Brillion zone start from X-axis to M. In this, the phase_x is fixed to 175 degree and phase_y is set start from 5 to 175 degree with step width 10 and the second set of DD is calculated.

3.10.3 M TO Γ

This is the last and final edge of the Brillion zone in which we equal phase_x with phase_y and set phase_x starts from 175 to 5 to complete the triangle of rectangular. The phase_y will remain same means 5, hence the last part of the DD is calculated (M to Γ). At the end all the data was export in ASIC form and then import for plotting diagram in MS Excel.

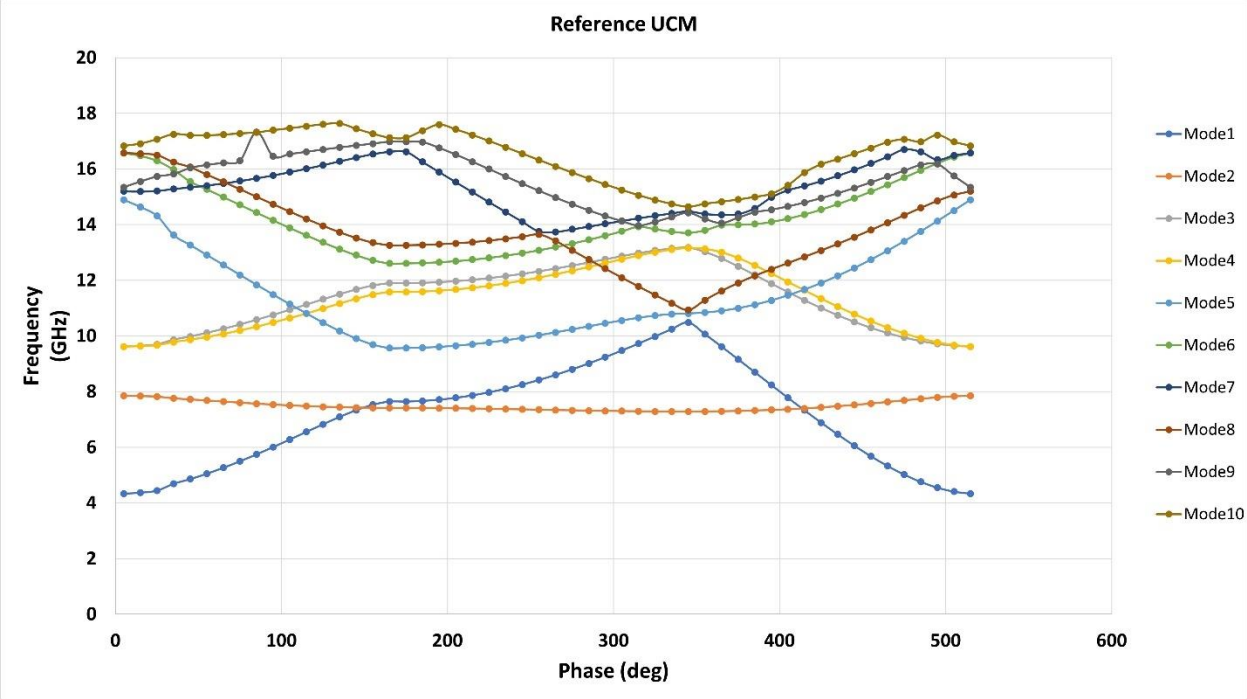

Figure 3.7 DD of Reference UCM Without Temperature

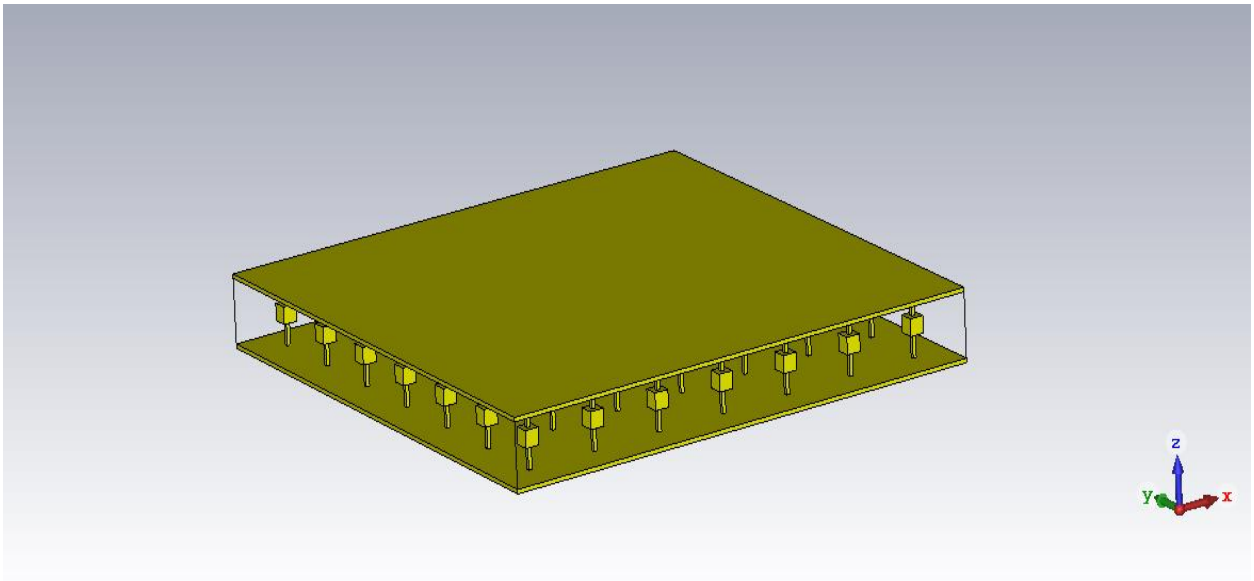

Figure 3.8 Array of Reference UCM

3.11 Unit Cell Model (With 250℃ Temperature)

This is the second part of the investigation of unit cell behavior but currently with assigning some sort of temperature by exploiting thermal solver analysis in Multiphysics (CST MPS).

Before utilizing Thermal solver analysis, coupled or co-simulation technique has been adopted for assigning temperature. Steps are as follows, first select schematic form the main window of the basic UCM as it can be seen in the figure 2-6 then select simulation project, after successful selection of simulation project, the "3D model as a block is selected" and another window will be open called "Create New Simulation Project" by selecting all necessary settings as can be seen in the figure project name, project type etc. Finally click "update" button the thermal simulation window will be created and also in the under Navigation Tree.

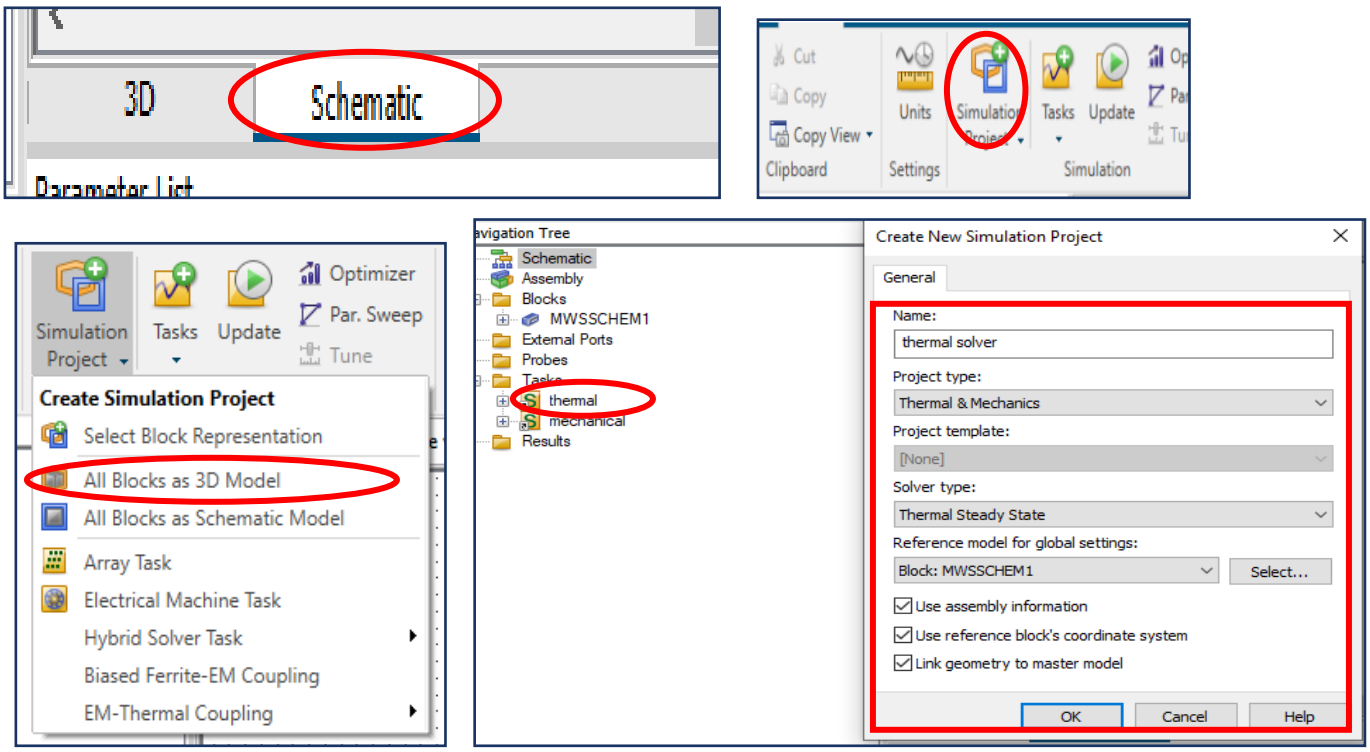

Figure 3.9 Set up for the thermal solver

After creating thermal simulation successfully, the thermal environment window will appear with the same UCM as it was in the EM solver, as the thermal solver has its own environment

along with thermal sources and many other features. Now set all the required setting like boundaries as “isothermal” in all the three dimensions, background as a “normal”, select “temperature source” from source and load, double click to the model and assign temperature value in kelvin, it is advisable to be in kelvin throughout the investigation. Now all the models will be covered by temperature source and become red as in the Fig 3.10.

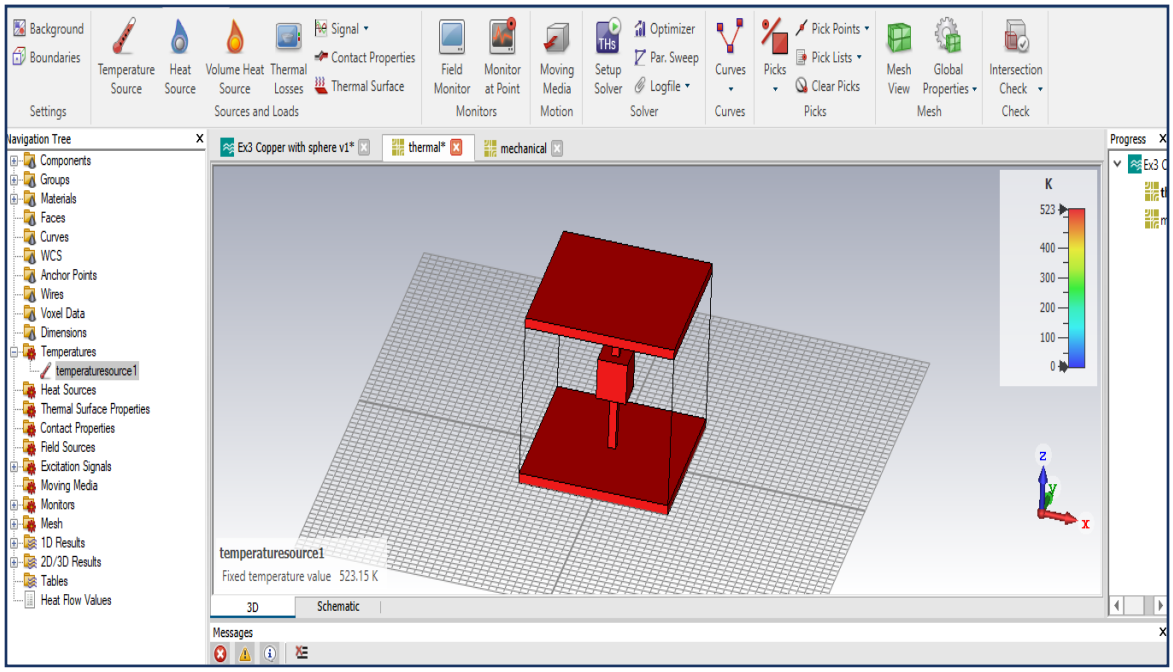

Figure 3.10 Thermal solver analysis

In thermal solver simulation, the value of the temperature assigned to the structure which is 523.15 K (250°C) and the ambient temperature set to 293.15 K (20°C)

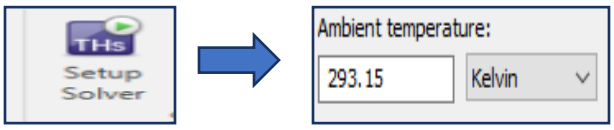

Figure 3.11 Setting Ambient temperature

After adopting all the necessary setting now click simulation button and the structure would be simulated successfully. Half part has been done, as the CTE is of interest so mechanical solver is needed because the CTE can be analyze only on in Mechanical Solver Analysis. To do so, all the

steps has been carried out as it was done during coupled simulation for thermal analysis in section 3.7 and figure 3.9 with a minor change, at this time, select “structural mechanic” instead of choosing “thermal steady state” see Fig 3.12.

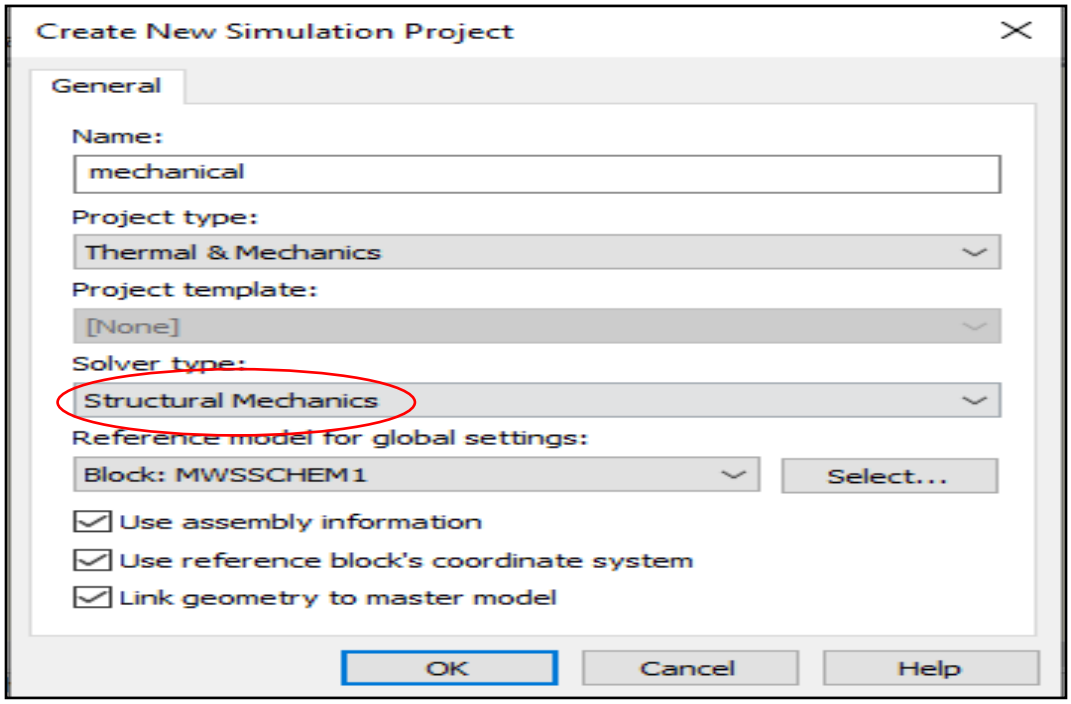

Figure 3.12 Mechanical setup solver

After creating the coupled mechanical simulation successfully, the new window would look like in Fig 3.12 with new mechanical setup solver.

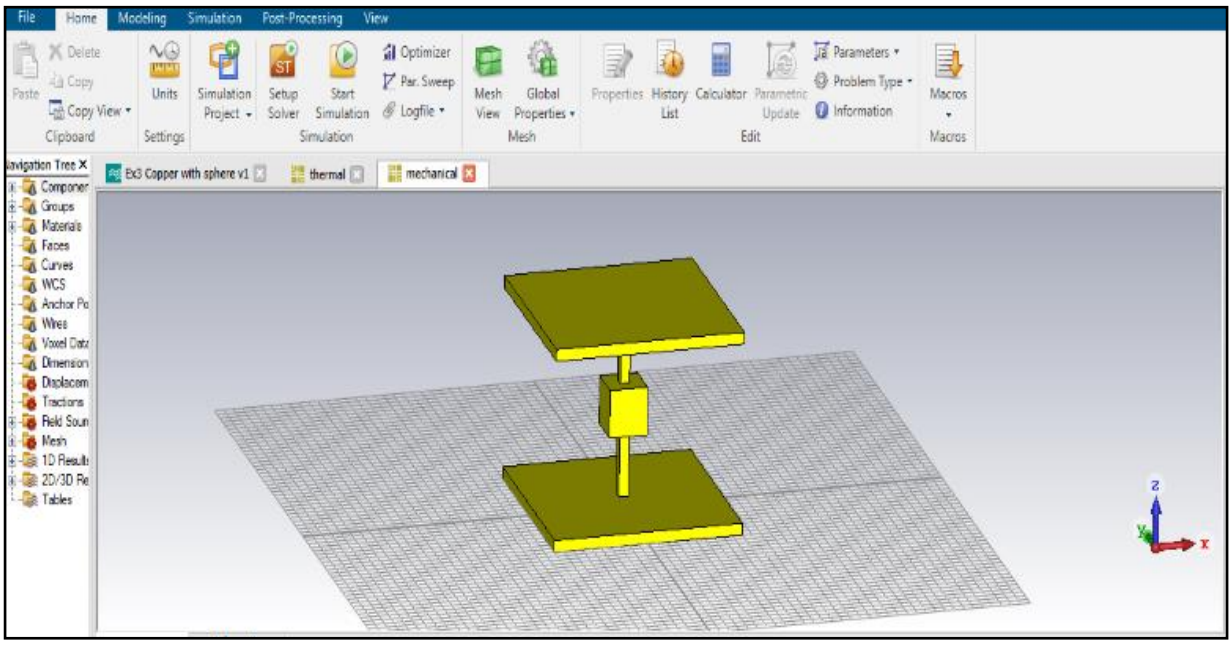

Figure 3.13 Coupled mechanical solver.

At this time, import the field from thermal simulation solver into mechanical, now follow the steps, click field import source then select “thermal “from project (remember to simulate thermal solver before setting the mechanical coupled simulation otherwise it would not be possible to import the field from thermal solver into mechanical) once the field has been imported successfully click setup solver to simulate structure. Once the simulation is done go to 2D/3D Results and select “Deformation” and tune a little bit with its properties to get result. Any ways finally, the thermally expended structure due to temperature looked like as in Fig 3.14. From the figures it can be seen clearly the effect of temperature on the specific structure cause thermal expansion as a result.

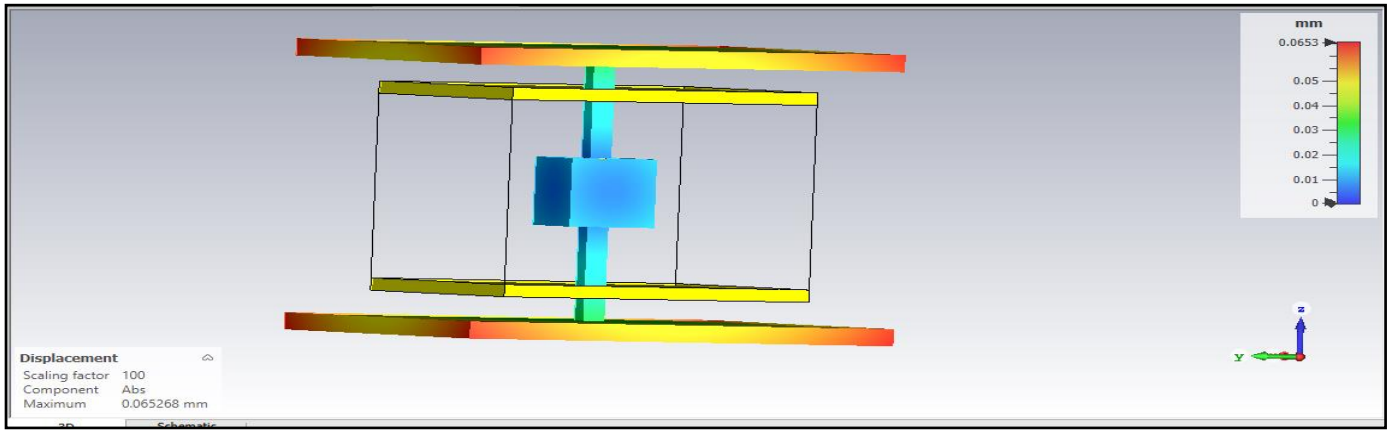

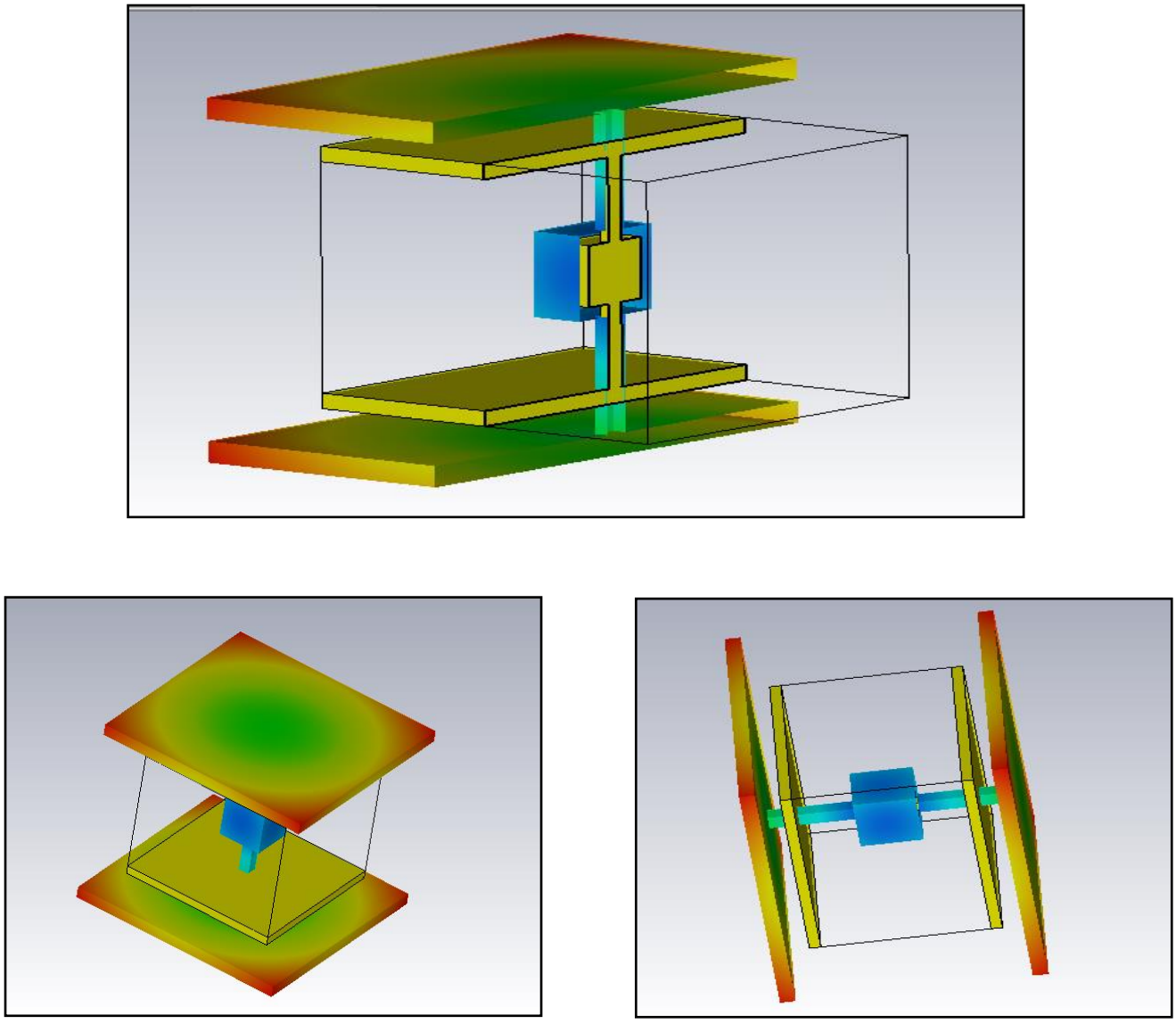

Figure 3.14 Thermally Expanded Structure due to Temperature source

Moreover, it can also be observed that the small structure is the main structure and the expended one is the bigger one. Not only this but also CTE can be observed numerically in the form of millimeter (mm) with respect to reference. The same model after expansion is Export as '**Mesh (STL)**'file format for the calculation of DD.

3.12 Importing Mesh (STL) Structure for DD

To calculate DD for 523.15 K (250℃) model, it is necessary to create new project in the high

frequency in EM solver and import the saved model name Mesh (STL) by drag and drop. Once the model is imported, change its material from default to copper and color see in Fig 2.12. Before calculating DD. It is necessary to heal the model to remove all the triangular, it can be done through **Modeling-Shape Tools-Heal All The Shapes**, for that the model would be look like as in the Fig 2.12.

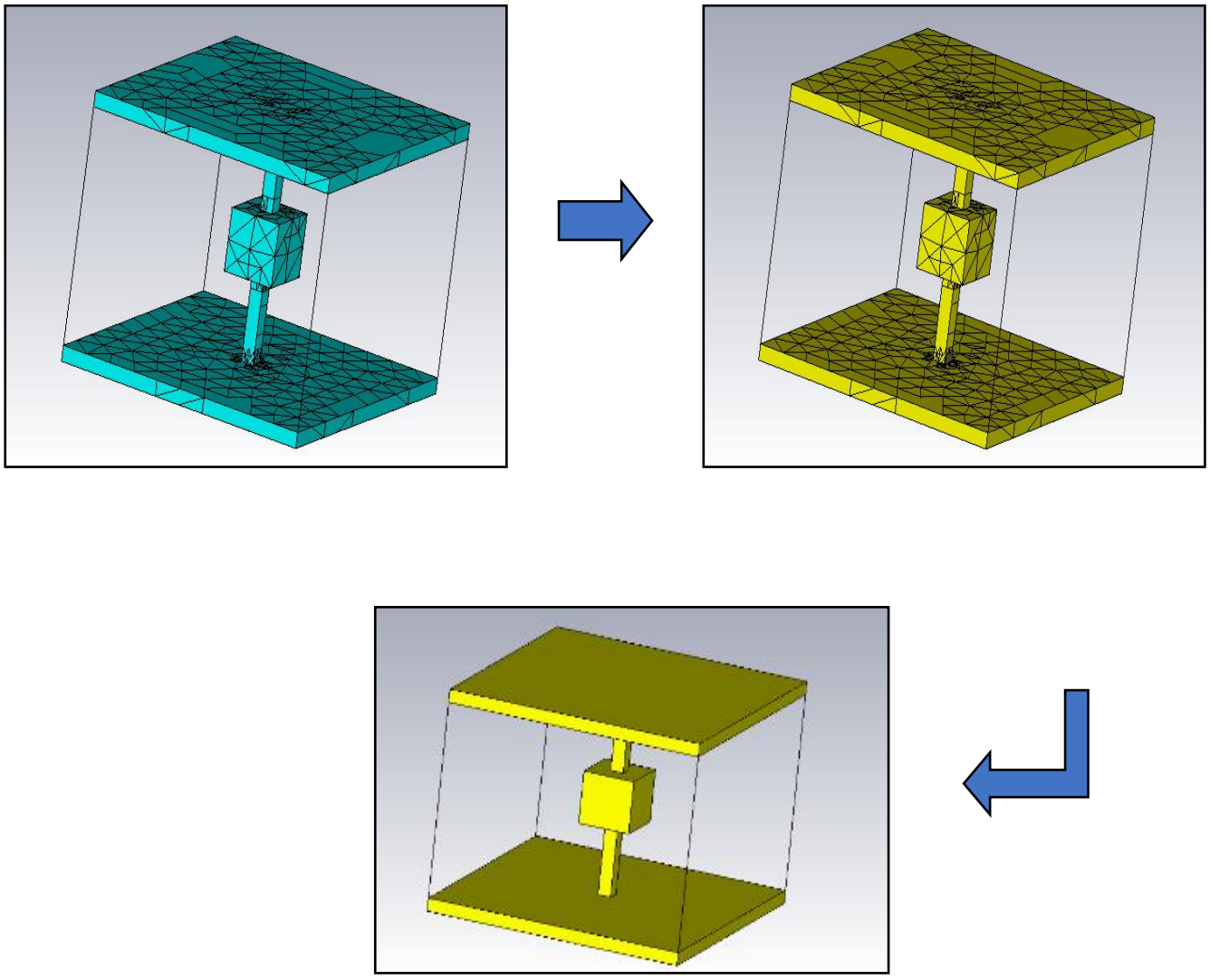

Figure 3.15 Imported Mesh (STL) Model

Now the DD is calculated for the UCM having 523.15 K (250℃).

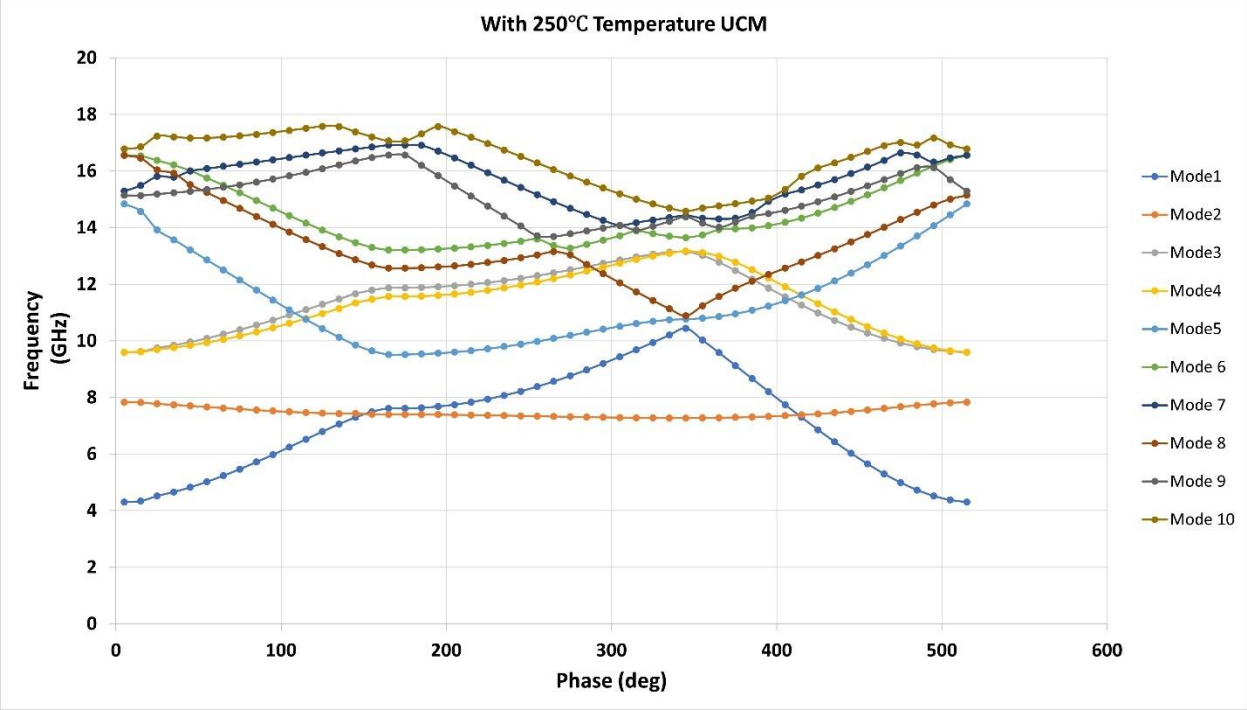

Figure 3.16 DD of UCM With 250℃ Temperature

3.13 Unit Cell Model (With 1200℃ Temperature)

For sure the above process mentioned in 3.6 section was used to calculate 523.15 K (250℃) temperature but can also be used to calculate different values of temperature as per requirement, so utilizing the same method as section 3.6 the UCM is evaluated for the temperature value of 1473.15 K (1200℃).

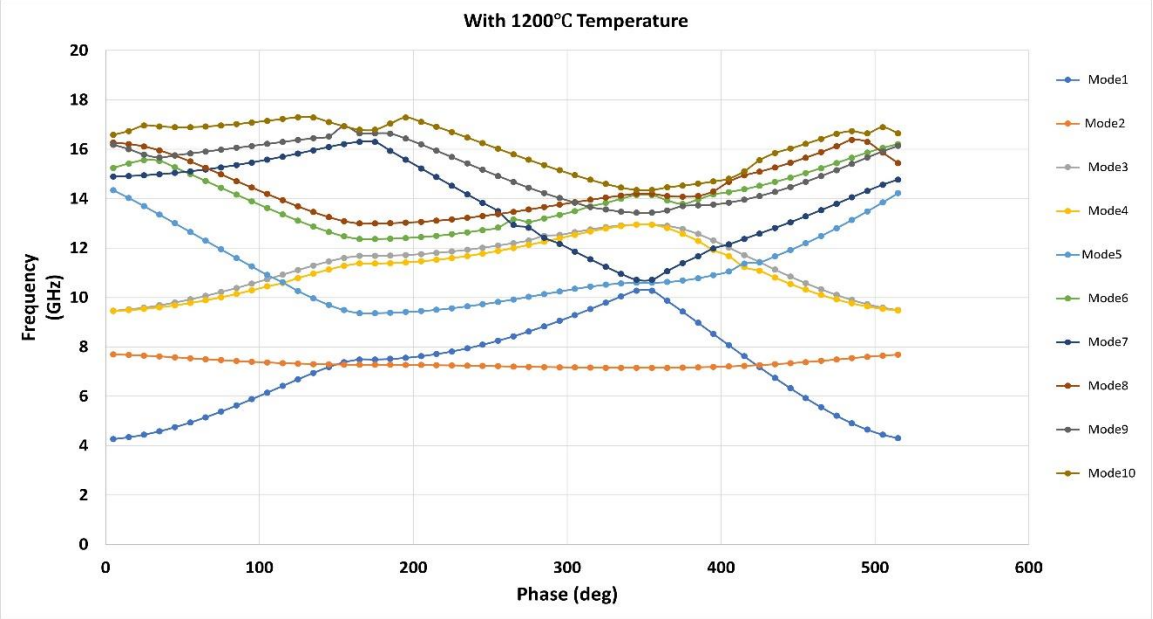

Figure 3.17 DD of UCM With 1200℃ Temperature

Chapter 4: Results and analysis

The impact of temperature source on the UCM causes the thermal expansion. The motivation of the thesis is to examine the rate of change occurred in terms of CTE in the UCM due to temperature provided. The analysis is carried out as follow, first the reference UCM structure is created in the CST MWS without assigning temperature and the DD is calculated by exploiting Brillion zone and its frequency band gap is observed as mentioned in chapter 3 and section 3.4. Moreover, its frequency band gap is observed through DD. After that, the UCM having temperature 250℃ is created and its DD is calculated, similarly the final UCM having very high value of temperature 1200℃ is created and its DD is calculated. All the UCMs are plotted on the same plot as a DD to see the changes. During the analysis it has been observed, the UCM with 250℃ is expend/increased 0.08mm as compared to reference UCM whereas the UCM having 1200℃ is expend more than 250℃ UCM almost 0.40mm.

4.1 Comparison of reference UCM with UCM 523.15 K (250℃)

By utilizing CST MPS feature of CST software, the value of temperature equal to 250℃ is applied to UCM, after simulation, the structure is thermally expended from its initial value. The difference can be seen in the table 4-1.

It can be seen clearly in the table 4-1 that the temperature is affecting UCM higher the temperature is, more the thermal expansion. At the value 523.15 K (250℃) the UTC is changed from initial reference or zero value to some tends of millimeter (mm). Moreover, plotting the DD of two-UCM (with 250℃ temperature and without temperature) combinedly, difference can be seen easily between two DD and stop band frequency can be observed.

Reference UCM		UCM with 250℃ Temperature
Grounded Square Plane and Top Square Plane (mm)		
Length	20	20.08
Width	20	20.08
Height	1.0	1.0

Via (connected ground to top) (mm)		
Length	1	1
Width	1	1
Height	15	15.06
Square Brick (connected with via) (mm)		
Length	4	4.02
Width	4	4.02
Height	4	4.02

Table 4-1 Dimension Comparison of initial UCM with 250℃ UCM

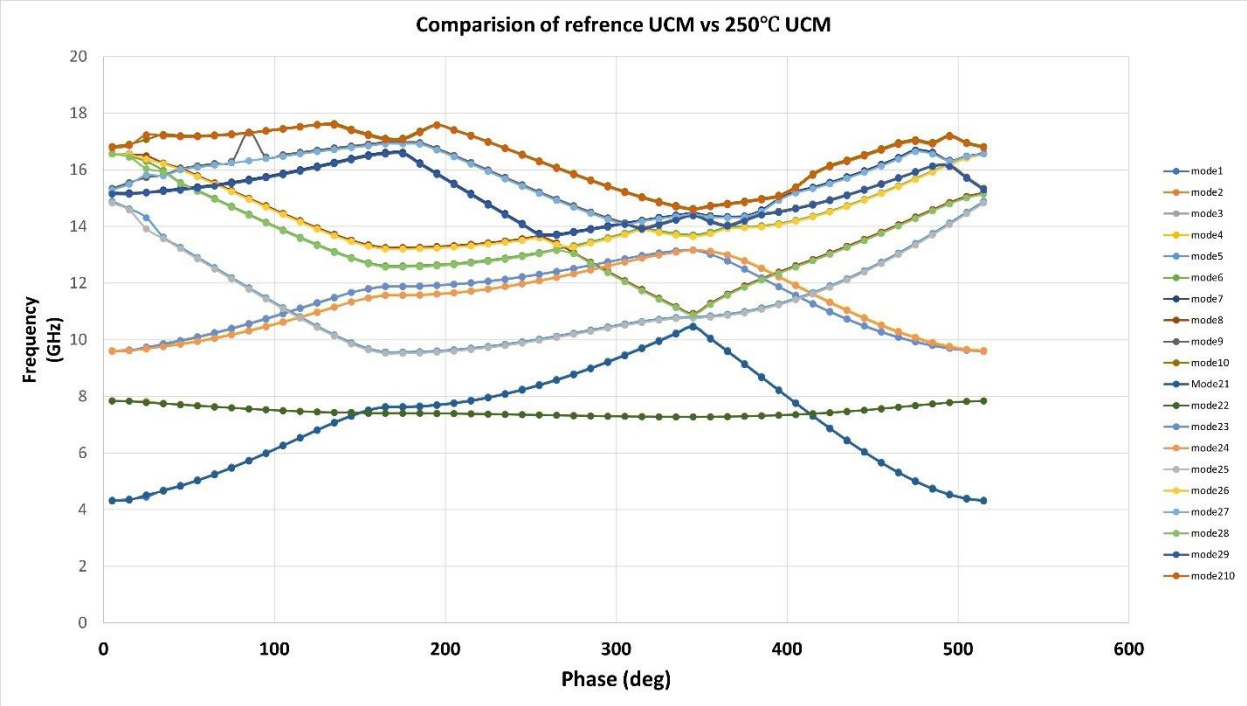

Figure 4.1 DD of reference UCM with 250℃ Temperature

4.2 Comparison of reference UCM with UCM at 1473.15 K (1200℃)

Reference UCM		UCM with 1200℃ Temperature
Grounded Square Plane and Top Square Plane(mm)		
Length	20	20.40
Width	20	20.40
Height	1.0	1.02
Via (connected ground to top) (mm)		
Length	1	1.02
Width	1	1.02
Height	15	15.30
Square Brick (connected with via) (mm)		
Length	4	4.08
Width	4	4.08
Height	4	4.08

Table 4-2 Dimension Comparison of Reference UCM with UCM 1200℃

The comparison of reference UCM with UCM at 1200℃ can be observed in the table Table 4-2,having such huge difference in the dimension it can be said that more the temperature is applied more the structure is expand, from the understating point of view, if square plates (bottom and top) of thermally expended structures is consider it can be seen that the length and width is increase at 0.08 mm at 250℃ and 0.40 mm at 1200℃ respectively with respect to reference UCM .

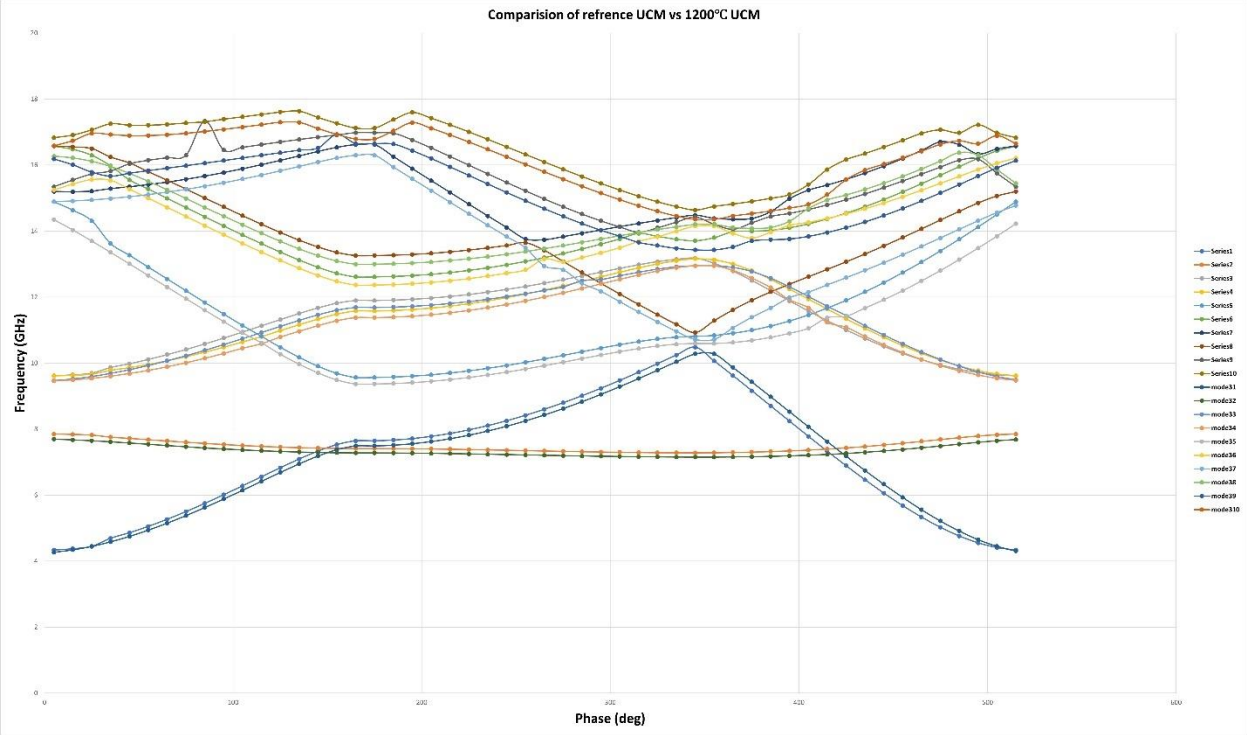

Figure 4.2 DD of reference UCM with 1200℃ Temperature

4.3 Comparison of reference UCM with UCM at 250℃ and 1200℃ respectively

UCM Without Temperature		UCM with 250℃ Temperature	UCM with 1200℃ Temperature
Grounded Square Plane and Top Square Plane(mm)			
Length	20	20.08	20.40
Width	20	20.08	20.40
Height	1.0	1.0	1.02
Via (connected ground to top)			
Length	1	1	1.02
Width	1	1	1.02
Height	15	15.06	15.30
Square Brick (connected with via)			
Length	4	4.02	4.08
Width	4	4.02	4.08
Height	4	4.02	4.08

Table 4-3 Dimension Comparison of all UCMs

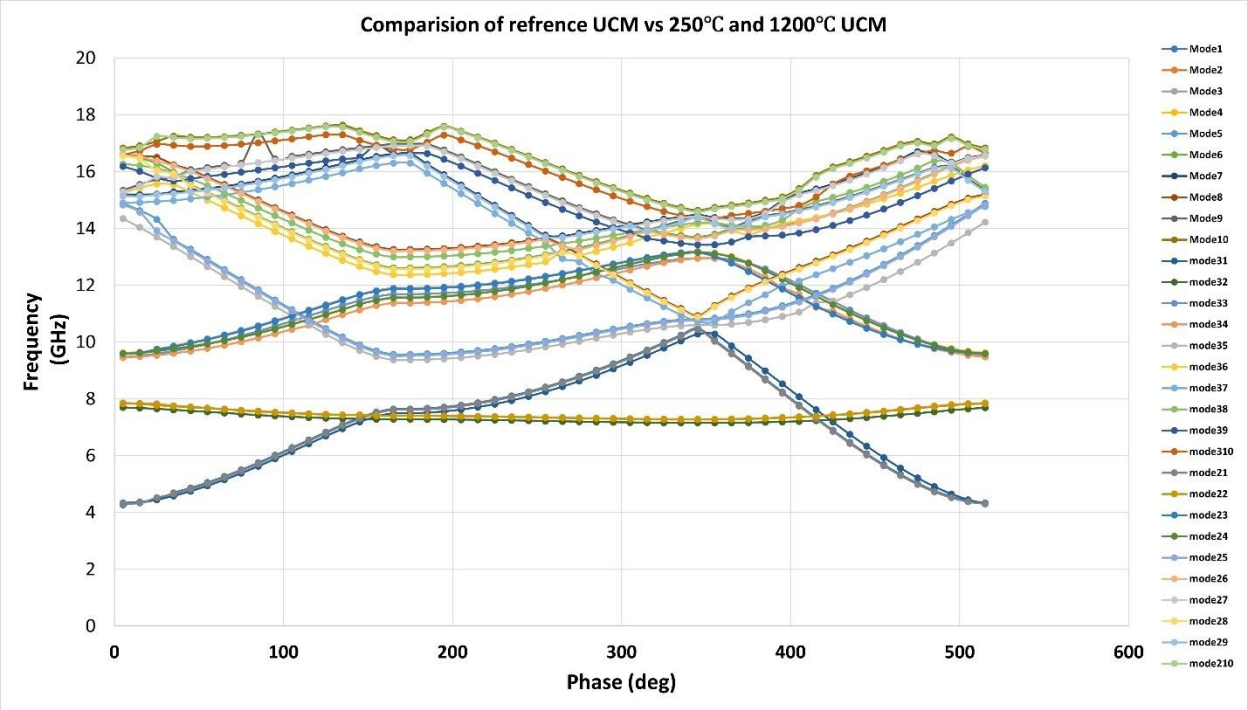

Figure 4.3 DD of initial UCM with 250℃ and 1200℃ UCM

4.4 Comparison of first mode of all UCMs

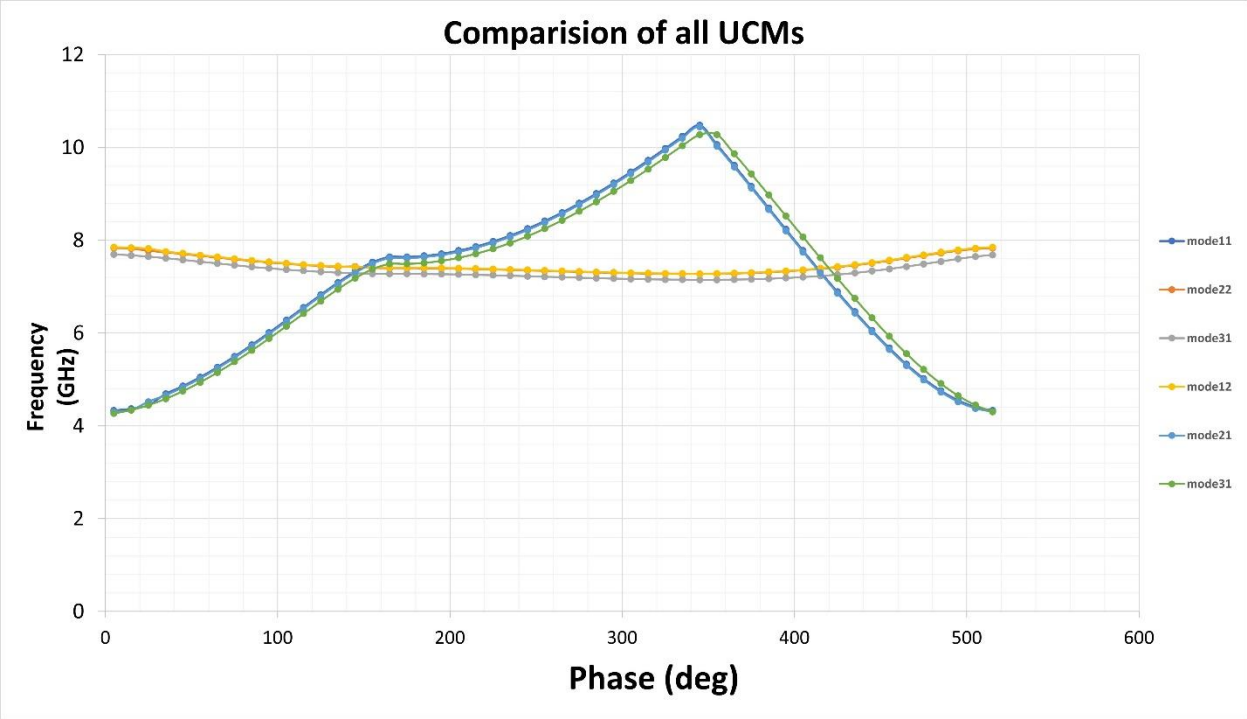

Figure 4.4 DD of all UCMs (only first two modes)

References

[1] Xu, L., Wen, Y., Pandit, S., Mokkapati, V., Mijakovic, I., Li, Y., . . . Liu, G. (2019). Graphene-based biosensors for the detection of prostate cancer protein biomarkers: a review.BMC Chem, 13(1), 112. doi:10.1186/s13065-019-0611-x

[2] Veselago, V. G. (1968). The Electrodynamics of Substances with Simultaneously Negative Values of Img Align= Absmiddle Alt= ϵ Eps/Img and μ. Physics-Uspekhi, 10(4), 509-514.

[03] Pendry, J. B., Holden, A. J., Robbins, D. J., & Stewart, W. (1999). Magnetism from onductors and enhanced nonlinear phenomena. IEEE transactions on microwave theory and techniques, 47(11), 2075-2084.

[04]Smith, D. R., et al. (2000). "Composite medium with simultaneously negative permeability and permittivity." Physical review letters 84(18): 4184.

[05] Pendry, J. B. (2000). "Negative refraction makes a perfect lens." Physical review letters 85(18): 3966.

[06] Smith, D. R. and N. Kroll (2000). "Negative refractive index in left-handed materials." Physical review letters 85(14): 2933.

[07] Oliveri, G., et al. (2015). "Reconfigurable electromagnetics through metamaterials—A review." Proceedings of the IEEE 103(7): 1034-1056.

[08] Alves, F., et al. (2013). "Bi-material terahertz sensors using metamaterial structures." Optics express 21(11): 13256-13271.

[09] Liu, J., et al. (2016). "Absorber: a novel terahertz sensor in the application of substance identification." Optical and Quantum Electronics 48(2): 80.

[10] Wilbert, D. S., et al. (2013). Terahertz metamaterials perfect absorbers for sensing and imaging.

[11] Carranza, I. E., et al. (2016). "Terahertz metamaterial absorbers implemented in CMOS technology for imaging applications: scaling to large format focal plane arrays." IEEE Journal of Selected Topics in Quantum Electronics 23(4): 1-8.

[12] Thongrattanasiri, S., et al. (2012). "Complete optical absorption in periodically patterned graphene." Physical review letters 108(4): 047401.

[13] Wang, L., et al. (2019). "Thermally tunable ultra-thin metamaterial absorber at P band." Journal of Electromagnetic Waves and Applications 33(11): 1406-1415.

[14,31] Huang, X., et al. (2019). "Thermally tunable metamaterial absorber based on strontium titanate in the terahertz regime." Optical Materials Express 9(3): 1377-1385.

[15] Nourbakhsh, M., Zareian-Jahromi, E., Basiri, R., & Mashayekhi, V. (2020). An Ultra-Wideband Terahertz Metamaterial Absorber Utilizing Sinusoidal-Patterned Dielectric Loaded Graphene. Plasmonics, 15(6), 1835-1843. doi:10.1007/s11468-020-01203-w
Oliveri, G., Werner, D. H., & Massa, A. (2015). Reconfigurable electromagnetics through metamaterials—A review. Proceedings of the IEEE, 103(7), 1034-1056.

[16] Elwi, T. A. (2019). Printed Microwave Metamaterial-Antenna Circuitries on Nickel Oxide Polymerized Palm Fiber Substrates. Sci Rep, 9(1), 2174. doi:10.1038/s41598-019-39736-8

[17] Wang, B., Zhou, J., Koschny, T., Kafesaki, M., & Soukoulis, C. M. (2009). Chiral metamaterials: simulations and experiments. Journal of Optics A: Pure and Applied Optics, 11(11), 114003. doi:10.1088/1464-4258/11/11/114003

[18] Yao, K., & Liu, Y. (2014). Plasmonic metamaterials. Nanotechnology Reviews, 3(2), 177-210. doi:doi:10.1515/ntrev-2012-0071.

[19] Feng, L., Huo, P., Liang, Y., & Xu, T. (2020). Photonic Metamaterial Absorbers: Morphology Engineering and Interdisciplinary Applications. Adv Mater, 32(27), e1903787. doi:10.1002/adma.201903787

[20] Fleisch, D. (2008). A Student's Guide to Maxwell's Equations: A Student's Guide to Maxwell's Equations.

[21] Iyer, A. K., & Eleftheriades, G. V. (2002). Negative refractive index metamaterials supporting 2-D waves. Paper presented at the 2002 IEEE MTT-S International Microwave Symposium Digest (Cat. No. 02CH37278).

[23] Pearson, A. M., Curry, R. D., & Noel, K. M. (2016). Characterization of double-positive metamaterials for advanced applications. Paper presented at the 2016 IEEE International Power Modulator and High Voltage Conference (IPMHVC).

[25] Engheta, N., & Ziolkowski, R. W. (2006). Metamaterials: physics and engineering explorations: John Wiley & Sons.
Farhat, M., Chen, P.-Y., Bagci, H., Amra, C., Guenneau, S., & Alù, A. (2015). Thermal invisibility based on scattering cancellation and mantle cloaking. Scientific Reports, 5(1), 1-9.

[26] Kriegler, C. E., Rill, M. S., Linden, S., & Wegener, M. (2009). Bianisotropic photonic metamaterials. IEEE Journal of Selected Topics in Quantum Electronics, 16(2), 367-375.

[27] Armstrong, C. M. (2012). The truth about terahertz. IEEE Spectrum, 49(9), 36-41.

[28] Williams, G. P. (2005). "Filling the THz gap—high power sources and applications." Reports on Progress in Physics 69(2): 301.

[29] Watts, C. (2015). Metamaterials and their applications towards novel imaging technologies. Boston College.

[30] Litchinitser, N. M., and V. M. Shalaev. "Photonic metamaterials." Laser Physics Letters 5.6 (2008): 411.

[32] Y. Dong and T. Itoh, "Metamaterial-Based Antennas," in Proceedings of the IEEE, vol. 100, no. 7, pp. 2271-2285, July 2012, doi: 10.1109/JPROC.2012.2187631

[33] Forouzmand, A. and A. B. Yakovlev (2015). "Electromagnetic cloaking of a finite conducting wedge with a nanostructured graphene metasurface." IEEE Transactions on Antennas and Propagation 63(5): 2191-2202.

[34] Smith, D. R. (2014). "A cloaking coating for murky media." Science 345(6195): 384-385.

[35] Farhat, M., et al. (2015). "Thermal invisibility based on scattering cancellation and mantle cloaking." Scientific Reports 5(1): 1-9.

[36] Haxha, S., AbdelMalek, F., Ouerghi, F. et al. Metamaterial Superlenses Operating at Visible Wavelength for Imaging Applications. Sci Rep 8, 16119 (2018).

[37] https://www.microwavejournal.com/articles/15980-cst-mphysics-studio#:~:text=CST%20MPHYSICS%20STUDIO%20(CST%20MPS,thermal%20and%20mechanical%20stress%20analysis.&text=The%20thermal%20solver%20can%20even,will%20interact%20with%20the%20body.